Discovery and Structure-Activity Relationships of Quinazolinone-2-carboxamide Derivatives as Novel Orally Efficacious Antimalarials

Journal of Medicinal Chemistry

pubs.acs.org/jmc

Article

Discovery and Structure−Activity Relationships of Quinazolinone-2-carboxamide Derivatives as Novel Orally Efficacious Antimalarials

Benoît Laleu,* Yuichiro Akao, Atsuko Ochida, Sandra Duffy, Leonardo Lucantoni, David M. Shackleford, Gong Chen, Kasiram Katneni, Francis C. K. Chiu, Karen L. White, Xue Chen, Angelika Sturm, Koen J. Dechering, Benigno Crespo, Laura M. Sanz, Binglin Wang, Sergio Wittlin, Susan A. Charman, Vicky M. Avery, Nobuo Cho, and Masahiro Kamaura

Cite This: https://doi.org/10.1021/acs.jmedchem.1c00441

Read Online

ACCESS | Metrics & More | Article Recommendations | Supporting Information

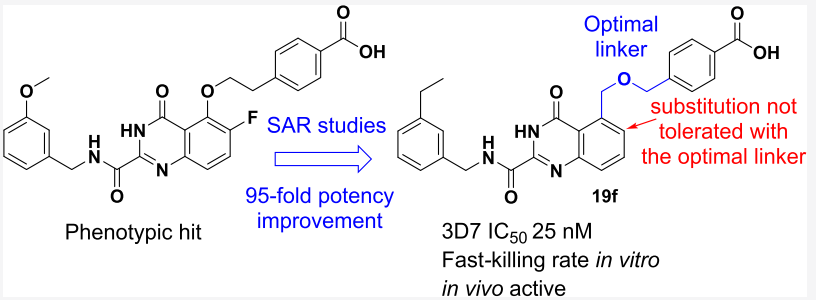

ABSTRACT: A phenotypic high-throughput screen allowed discovery of quinazolinone-2-carboxamide derivatives as a novel antimalarial scaffold. Structure−activity relationship studies led to identification of a potent inhibitor **19f**, 95-fold more potent than the original hit compound, active against laboratory-resistant strains of malaria. Profiling of **19f** suggested a fast *in vitro* killing profile. *In vivo* activity in a murine model of human malaria in a dose-dependent manner constitutes a concomitant benefit.

INTRODUCTION

Malaria is a mosquito-borne disease that remains a critical public health challenge in the world with 229 million cases of malaria and 409 000 deaths reported in 2019.[1] Human malaria is caused by five different species of parasites belonging to the *Plasmodium* genus, with *Plasmodium falciparum* being the most lethal species. The rise of resistance to current antimalarial drugs, including artemisinin combination therapies (ACTs), threatens efforts toward malaria elimination and eradication.[1−3] This underscores the need to discover chemotypes with novel modes of action active against resistant parasites to replace or combine with existing malaria medicines.[4−6] In that regard, antimalarial hit and lead criteria as well as target candidate profiles have been established to define the attributes that need to be demonstrated by new antimalarial molecules.[7,8]

Herein, we describe the identification of a novel antimalarial scaffold. Structure−activity relationship (SAR) studies allowed one to achieve 95-fold improvement of potency from the hit compound with identification of a potent inhibitor demonstrating *in vivo* efficacy in a humanized SCID mouse model of *P. falciparum* malaria.

RESULTS AND DISCUSSION

Hit Identification. In search for novel antimalarials, a Takeda proprietary library of 20 064 compounds, designed to maximize structural diversity (molecular weight: range 107−1449 g/mol, mean 390 g/mol; cLog *P*: range −8.91 to 10.44, mean 3.61; cLog *D* at pH 7.4: range −9.71 to 10.17, mean 2.99; sp3 character: range 0.00−1.00, mean 0.287), was screened against *P. falciparum* using a phenotypic growth inhibition assay.[9] As the most potent hit series were previously abandoned, we retrospectively re-evaluated the results of the HTS to rescue hits with potency in the micromolar range that appeared readily chemically tractable and possessed favorable physicochemical properties. Among those, compound **1** (ligand efficiency and lipophilic efficiency of 0.21 and 3.45, respectively) caught our attention since it was previously reported by Takeda as a selective matrix metalloproteinase (MMP)-13 inhibitor[10] and exhibited acceptable physicochemical properties (e.g., calculated Log *D* at pH 7.4 = 2.01, molecular weight 491.5) and lipophilic efficiency (LipE). Resynthesis allowed activity confirmation from a fresh solid sample, with no significant shift against the resistant malaria strain Dd2 (IC_{50} values of 2.38

Received: March 10, 2021

and 4.46 μM against 3D7 and Dd2, respectively) and no cytotoxicity observed against HEK293 mammalian cells (Figure 1).

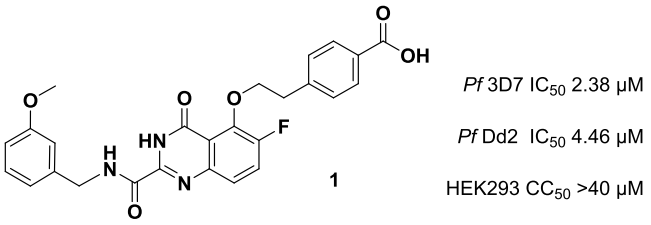

Figure 1. Antimalarial hit compound **1**.

The most frequent side effect associated with the clinical trials of MMP inhibitors was reported to be a musculoskeletal syndrome (MSS) that manifested as pain and immobility in the shoulder joints, arthralgias, and contractures in the hands. MMP-1, 2, and 14 were prime candidates as the possible causes of MSS but with no definitive answer.[11] It has been recently demonstrated that selective MMP inhibitors targeting MMP-2, MMP-9, or MMP-13 were not involved in MSS.[12] Until the possible relationship between MSS and inhibition of MMP-1 and -14 is fully explained, avoiding the use of this class of MMP inhibitors in chronic scenarios seems wise. Given this uncertainty and the short antimalarial treatment dosing timeframe, greater than 100-fold selectivity against MMP-1 and -14 was arbitrarily set as the ultimate goal for a potential clinical candidate. As the hit compound **1** was initially designed as a selective MMP-13 inhibitor (IC_{50} 0.0039 nM, >41 000-fold selectivity over other MMPs) and benefits from low inhibitory activity against MMP-1 and -14 (IC_{50}s > 10 μM),[10] we decided to profile this chemical series against MMP-1 and MMP-14 at a later stage while focusing on antimalarial treatment (and not prophylaxis) as a possible indication.

Despite modest potency, the absence of a significant shift against Dd2 and the therapeutic index against HEK293 cells suggesting the absence of obvious safety flags around MMP-13 inhibition encouraged us to evaluate this chemical class further.

Chemistry. As close structural analogues previously reported[10] as MMP-13 inhibitors covered modifications of the acidic part (*vide infra*, Table 1, compounds **2** and **3**), initial synthetic efforts were directed toward the left-hand side (LHS) of the molecule. This part appeared indeed readily amenable to a variety of modifications through introductions of various amines. To establish rudimentary structure−activity relationships (SARs), quinazolinone-2-carboxamide derivatives of type **9** were prepared following a slightly modified procedure of the one previously reported[10] (Scheme 1). The synthetic route was not optimized, with emphasis on purity of the product rather than quantity. Chemical diversity was introduced in the fourth step, by varying the amine moieties to be introduced, before conducting nucleophilic aromatic substitution with 4-(2-hydroxyethyl)benzoic acid to yield the final compounds **9a−m** (see Table 1 for more details).

As **9h** was identified as the potent derivative among the ones tested, condensation with ammonium chloride or ethylamine was performed to give amide derivatives **10a** and **10b** to probe further the essentiality of the acidic functional group (Scheme 2).

Once the potential optimal LHS was identified, the linker between the quinazolone core and the acidic moiety was thoroughly investigated, as well as the influence of substituents on the phenyl moiety of the quinazolone ring (Scheme 3). The appropriate nitrobenzoic acid of type **11** (**aa−ah**) was used as the starting material and readily converted into the corresponding methyl ester **12aa−ah** following standard methods. Bromination was then performed using 1,3-dibromo-5,5-dimethyl-imidazolidine-2,4-dione (DBMH) or *N*-bromosuccinimde (NBS)[13] with benzoyl peroxide (BPO) or 2,2-azobis-(isobutyronitrile) (AIBN) as the radical initiator to afford intermediates **13aa−ah**. At this stage, bromine displacement by a variety of nucleophiles of type **14** (alcohols, phenols, amines, or thiols) was performed under the appropriate reaction conditions. This allowed the coverage of a broad range of different spacers with alteration of both chain length and functionality with intermediates **15a−n**. Reduction of the nitro group followed by saponification generated anthranilic acids **17a−n**. The following step consisted of a condensation reaction with ethyl cyanoformate to give quinazolinones **18a−n**. Finally, the ester at the 2-position was reactive enough for introduction of (3-ethylphenyl)methanamine in the presence of triethylamine to afford quinazolinone-2-carboxamides **19a−n** in 9−30% overall yields.

Next, we decided to alter the position of the carboxylic acidic functionality on the optimal linker (compound **19o**) as well as the site of linkage onto the quinazolinone ring (**19p−r**). Synthetic routes followed the one used in Scheme 3, with the main modification being the use of silver oxide to force the displacement of the bromine by the appropriate hydroxymethylbenzoic acid in the third step[14] (Scheme 4).

Having determined the potential optimal linker, we synthesized a few compounds by varying the LHS of the molecule. Starting from intermediate **15f**, benzylamines were readily introduced to afford compounds **20a−g** (Scheme 5, *vide infra* Table 3 for more details) in excellent yields (91−96%). An amide derivative of **19f** was also synthesized following standard conditions (compound **21**, Scheme 6).

Antiplasmodial Activity and Cytotoxicity Assessment. All compounds were tested in a phenotypic 72 h growth inhibition assay for *P. falciparum*[9] (3D7 strain) and a 72 h HEK293 assay[15] to assess the intraerythrocytic antiplasmodial activity and mammalian cytotoxicity, respectively. Activity against the Dd2 strain was determined only for key compounds to ensure no obvious concern against resistance (mutated loci: *Pf*crt, *Pf*mdr1, *Pf*dhfr, and *Pf*dhps; choloroquine-, mefloquine-, pyrimethamine-, and sulfadoxine-resistant, respectively). Pyrimethamine, chloroquine, artesunate, DHA, and puromycin were used as reference antimalarial drugs in each *P. falciparum* growth inhibition assay run. None of the compounds showed any sign of cytotoxicity (CC_{50} > 20 μM) against HEK293 mammalian cells. For clarity, these cytotoxicity data were not included in the SAR Tables.

STRUCTURE−ACTIVITY RELATIONSHIPS

SAR on the Left-Hand Side. Our primary goal was to establish rudimentary SAR around the hit scaffold. Data on a representative set of compounds are summarized in Table 1. Initially, the need for the acidic moiety was investigated. Removal of this functionality (compound **2**) or its replacement by an aniline (compound **3**) resulted in complete loss of antiplasmodial activity, whereas subnanomolar potencies were reported with respect to human MMP-13 inhibition.[10] These results highlight the importance of the carboxylic acid for antiplasmodial potency and discouraged us from immediate

https://doi.org/10.1021/acs.jmedchem.1c00441
J. Med. Chem. XXXX, XXX, XXX−XXX

Table 1. Antiplasmodial Rudimentary SAR around the Left-Hand Side (R^1 and R^2 Modifications)

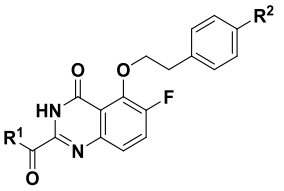

Cpd	R^1	R^2	IC_{50} (μM)[a]	CI or SD (μM)[b]	Cpd	R^1	R^2	IC_{50} (μM)[a]	CI or SD (μM)[b]
2	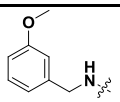	H	>20	NA	**9h**	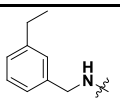	COOH	0.42[c]	±0.16
3	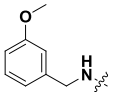	NH_2	>20	NA	**9i**	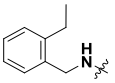	COOH	>20	NA
9a	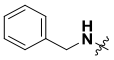	COOH	3.67	2.75-4.91	**9j**	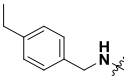	COOH	1.16	0.94-1.44
9b	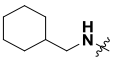	COOH	>20	NA	**9k**	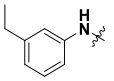	COOH	3.19	2.72-3.74
9c	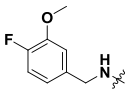	COOH	1.90	1.58-2.28	**9l**	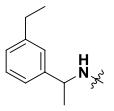	COOH	5.13	3.48-7.55
9d	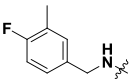	COOH	0.59	0.46-1.01	**9m**	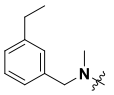	COOH	>20	NA
9e	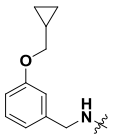	COOH	1.67	1.36-2.05	**10a**	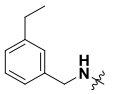	$CONH_2$	>20	NA
9f	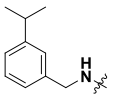	COOH	1.16	0.99-1.35	**10b**	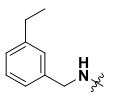	CONHEt	>20	NA
9g	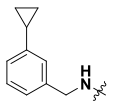	COOH	4.76	3.59-6.32					

[a]$N = 1$ (unless otherwise specified), duplicate points against *Pf* 3D7 (DAPI 72 h inhibition growth assay); compound **9h** was used as the internal control when testing compounds **9i−m** and **10a,b**; antimalarial drugs pyrimethamine, chloroquine, artesunate, DHA, and puromycin were used as references (mean IC_{50} values of 0.009, 0.025, 0.001, 0.0004, and 0.077 μM, respectively) in all experiments. [b]Confidence interval or standard deviation; NA, not applicable. [c]Mean value, $N = 9$, duplicate points.

additional investigations targeting this part of the molecule. The data suggested possible SAR divergence between activity against malaria parasites and human MMP-13 inhibition.

To generate rudimentary SAR in a short timeframe, close structural analogues of the hit compound (**9a−m**) were synthesized through variations of the LHS while fixing R^2 = COOH. The influence of R^1 substitution started with evaluation of the unsubstituted benzyl derivative (**9a**) and its cyclohexyl structural analogue (**9b**). **9a** demonstrated activity in the same range as the antiplasmodial hit, indicating a most likely marginal effect of the methoxy substituent on potency. This corroborated further the hypothesis of divergent SAR between human MMP-13 inhibition and antiplasmodial activity. In contrast, the inactivity of **9b** underscored the importance of the LHS benzyl group, which encouraged us to investigate its substitution pattern. Methyl (**9d**) or a larger alkoxy group (**9e**) appeared to be beneficial over the methoxy substituent harbored by the original hit. These findings directed us toward further

https://doi.org/10.1021/acs.jmedchem.1c00441
J. Med. Chem. XXXX, XXX, XXX−XXX

Scheme 1. Synthesis of Quinazolinone-2-Carboxamides 9a−m[a]

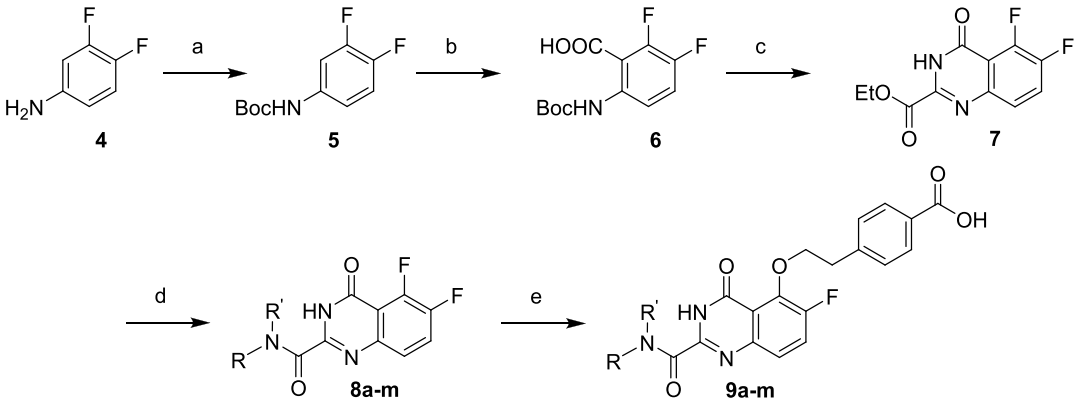

[a]Reagents and conditions: (a) Boc_2O, THF, 60 °C; (b) s-BuLi, CO2, THF, −78 °C; (c) CNCOOEt, HCl/dioxane, 80 °C; (d) RR′NH, $AlMe_3$, toluene, 0−25 °C; (e) 4-(2-hydroxyethyl)benzoic acid, NaH, DMF, 25 °C; then, 60−80 °C.

Scheme 2. Synthesis of Amides 10a and 10b[a]

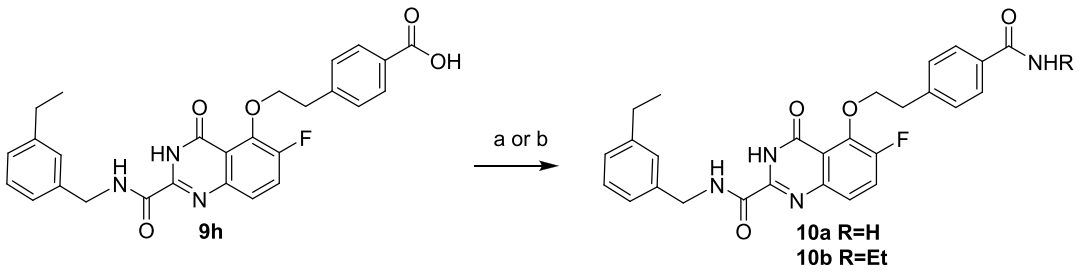

[a]Reagents and conditions: (a) DIEA, NH_4Cl, HATU, CH_3CN, 25 °C; (b) DIEA, ethylamine, HATU, CH_3CN, 20 °C.

Scheme 3. Synthesis of Quinazolinone-2-Carboxamides 19a−n[a]

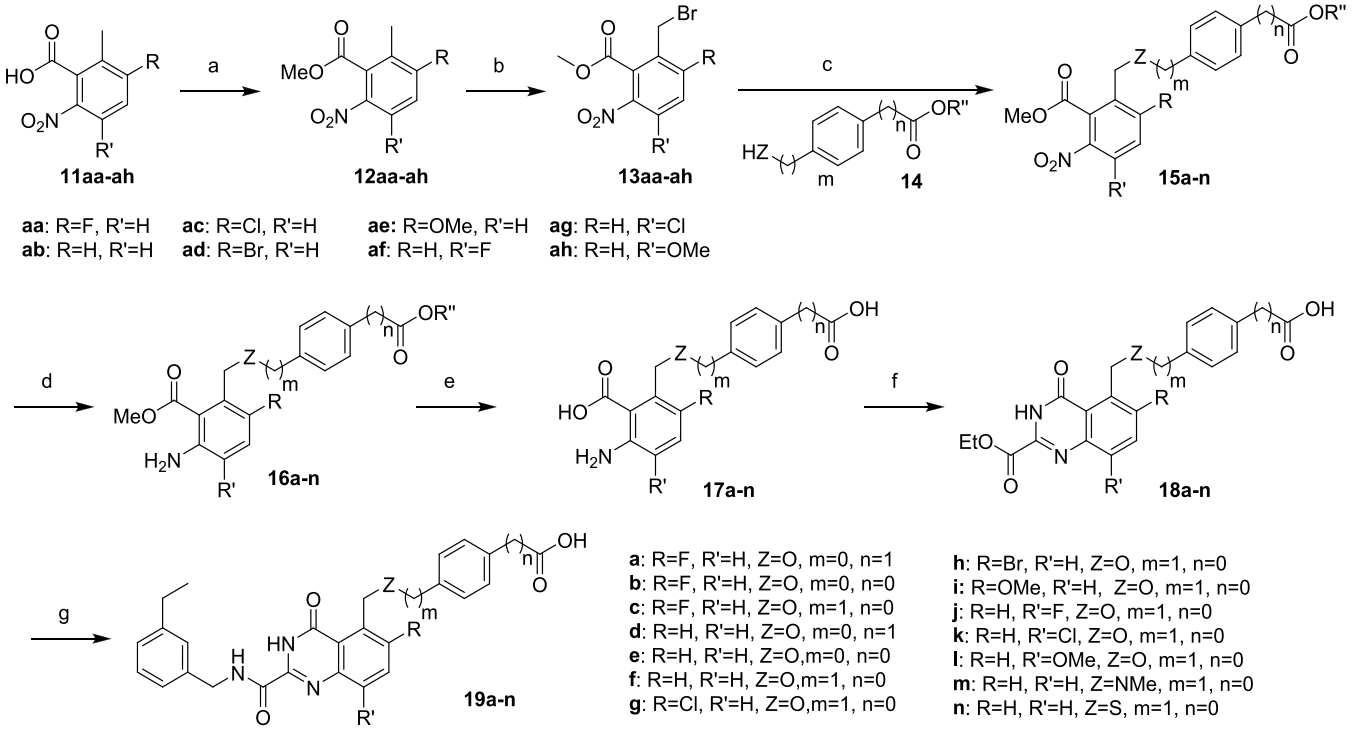

[a]Reagents and conditions: (a) Method A: $SOCl_2$, CH_3OH; Method B: K_2CO_3, CH_3I; (b) Method A: DBDMH, BPO; Method B: DBDMH, AIBN; (c) Method A: K_2CO_3; Method B: NaH; (d) Fe, NH_4Cl; (e) Method A: NaOH, CH_3OH/H_2O; Method B: LiOH, CH_3OH/H_2O; (f) CNCOOEt, HCl/dioxane; (g) Et_3N, (3-ethylphenyl)methanamine.

https://doi.org/10.1021/acs.jmedchem.1c00441
J. Med. Chem. XXXX, XXX, XXX−XXX

Scheme 4. Synthesis of Quinazolinones of Types 19o−r[a]

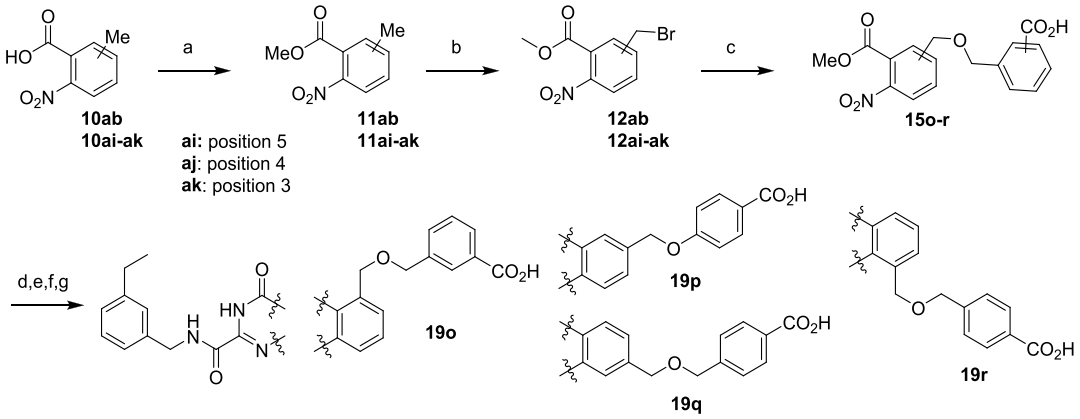

[a]Reagents and conditions: (a) Method B: K_2CO_3, CH_3I; (b) Method B: DBDMH, AIBN; (c) Method C: Ag_2O, 3-(hydroxymethyl)benzoic acid or 4-(hydroxymethyl)benzoic acid; (d) Fe, NH_4Cl; (e) Method B: LiOH, CH_3OH/H_2O; (f) CNCOOEt, HCl/dioxane; (g) Et_3N, (3-ethylphenyl)methanamine.

Scheme 5. Synthesis of Compounds of Types 20a−e[a]

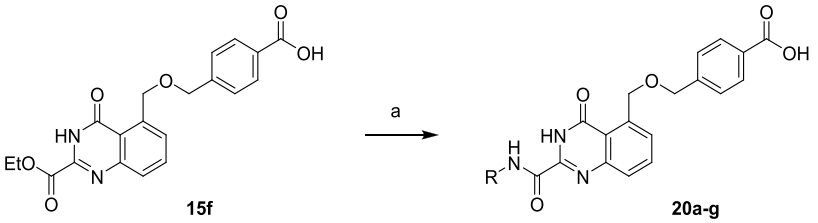

[a]Reagents and conditions: (a) RNH_2 (3 equiv.), Et_3N, EtOH, 50 °C.

Scheme 6. Synthesis of Compound 21[a]

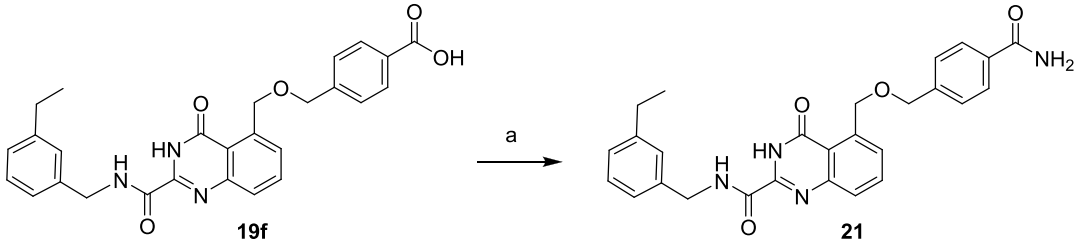

[a]Reagents and conditions: (a) DIEA, NH_4Cl, EDCI, CH_3CN, 25 °C.

exploration of alkyl substituents by varying their size and length (**9f−h**). Among those, *meta*-ethyl revealed to be the best substituent with 5.7-fold improvement in potency when compared to the hit compound (**9h** *vs* **1**). It appeared therefore logical to alter the position of this ethyl substituent on the benzyl moiety (**9i,j**). *para*-Substitution was relatively well-tolerated, whereas *ortho*-substitution resulted in complete loss of inhibitory effect. Compound **9k**, the aniline analogue of **9h**, showed ∼7-fold loss of potency. On the other hand, incorporation of a methyl group at the benzylic position (**9l**) or on the amine nitrogen (**9m**) gave disappointing results. Finally, amide derivatives **10a** and **10b** of the most potent compound **9h** were found to be totally inactive, which reinforced the initial findings with respect to the need for the carboxylic acid moiety.

In summary, this initial SAR investigation shed light on the *meta*-ethylbenzylamine moiety as being the potential optimal LHS. SAR data suggest involvement of this alkyl substituent in van der Waals and/or hydrophobic interactions with associated steric constraints. The submicromolar potency demonstrated by **9h** was further confirmed by testing against the Dd2-resistant strain (IC_{50} values of 0.42 and 0.21 μM against 3D7 and Dd2, respectively), which convinced us to pursue investigation on this chemotype as a novel antimalarial scaffold.

SAR on the Right-Hand Side. After probing the SAR on the LHS, we next turned our attention toward the linker between the quinazolinone ring and the acidic function. A variety of spacers was evaluated while fixing the LHS as *meta*-ethylbenzylamine to allow direct comparison with **9h**. Results are presented in Table 2.

Initially, R^4 was set as fluorine. Modifications focused on walking the ether oxygen atom and altering the length of the linker not only between the quinazolinone and the phenyl but also between the phenyl and the carboxylic acid moiety. All tested changes (**19a−c**) were found detrimental. Despite these disappointing results, the same variations were considered with R^4 = H. While compounds **19d−e** were found to be totally inactive, **19f** showed double-digit nanomolar potency (3D7 IC_{50}

https://doi.org/10.1021/acs.jmedchem.1c00441
J. Med. Chem. XXXX, XXX, XXX−XXX

Table 2. Antiplasmodial SAR: Linker and Right-Hand-Side Investigation (R^3, R^4, R^5, R^6 Modifications)

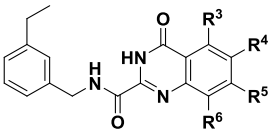

Cpd	R^3	R^4	R^5	R^6	IC_{50} (μM)[a]	CI or SD (μM)[b]
19a	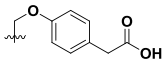	F	H	H	>20[c]	NA
19b	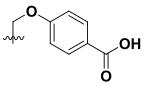	F	H	H	6.97	*d*
19c	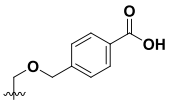	F	H	H	4.46	3.49-5.69
19d	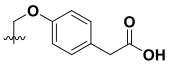	H	H	H	>20[c]	NA
19e	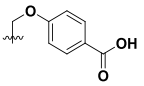	H	H	H	>20	NA
19f	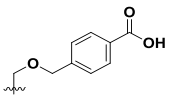	H	H	H	0.025[e]	±0.027
19g	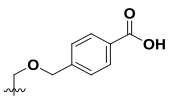	Cl	H	H	>20	NA
19h	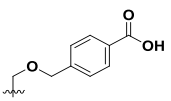	Br	H	H	>20	NA
19i	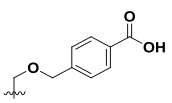	OMe	H	H	>20	NA
19j	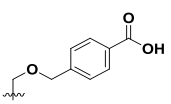	H	H	F	0.054	0.020-0.088
19k	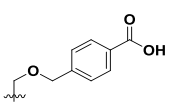	H	H	Cl	0.16	0.13-0.19
19l	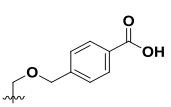	H	H	OMe	1.89	1.72-2.09
19m	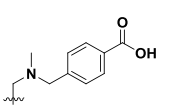	H	H	H	1.15	0.95-1.40

https://doi.org/10.1021/acs.jmedchem.1c00441
J. Med. Chem. XXXX, XXX, XXX−XXX

Table 2. continued

19n	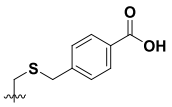	H	H	H	5.54[c]	±0.59
19o	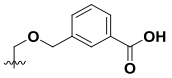	H	H	H	1.58	1.26-1.99
19p	H	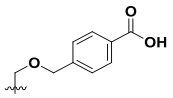	H	H	1.62	1.43-1.82
19q	H	H	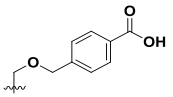	H	>20	NA
19r	H	H	H	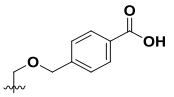	>20	NA

[a]N = 1 (unless otherwise specified), duplicate points against *Pf* 3D7 (DAPI 72 h inhibition growth assay); compound **9h** was used as the internal control when testing compounds **19a−f**; compound **19f** was used as the internal control when testing compounds **19g−r**; antimalarial drugs pyrimethamine, chloroquine, artesunate, DHA, and puromycin used as references (mean IC_{50} values of 0.008, 0.035, 0.0004, 0.0002, and 0.108 μM, respectively) in all experiments. [b]Confidence interval or standard deviation; NA, not applicable. [c]Mean value, N = 2, duplicate points. [d]Curve too steep to get confidence limits. [e]Mean value, N = 13, duplicate points.

Table 3. Antiplasmodial SAR with Potential Optimal Linker (R^1 and R^2 Modifications)

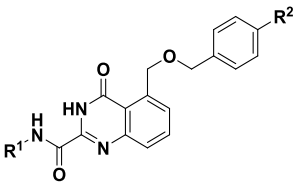

Cpd	R^1	R^2	IC_{50} (μM)[a]	CI or SD (μM)[b]	Cpd	R^1	R^2	IC_{50} (μM)[a]	CI or SD (μM)[b]
20a		COOH	0.18[c]	±0.067	**20e**	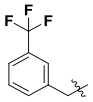	COOH	0.41	0.36-0.47
20b		COOH	0.28	0.24-0.33	**20f**		COOH	0.89	0.60-1.32
20c	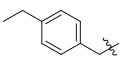	COOH	0.073	0.060-0.087	**20g**		COOH	0.55	0.43-0.66
20d	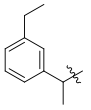	COOH	5.94	2.64-13.3	**21**		$CONH_2$	0.31	0.22-0.44

[a]N = 1 (unless otherwise specified), duplicate points against *Pf* 3D7 (DAPI 72 h inhibition growth assay); compound **19f** (mean IC_{50} 0.025 μM) was used as the internal control; antimalarial drugs pyrimethamine, chloroquine, artesunate, DHA, and puromycin were used as reference controls (mean IC_{50} values of 0.006, 0.028, 0.0006, 0.0003, and 0.087 μM, respectively) in all experiments. [b]Confidence interval or standard deviation. [c]Mean value, N = 6, duplicate points.

= 25 nM). Remarkably, this constituted a 378- and 95-fold improvement in potency versus its fluorinated analogue **19c** and the original hit **1**, respectively. Such a dramatic impact was not observed with respect to human MMP-13 SAR.[10] Surprised by the huge difference in activity between **19c** and **19f**, we decided to test close structural analogues by varying substituents at

https://doi.org/10.1021/acs.jmedchem.1c00441
J. Med. Chem. XXXX, XXX, XXX−XXX

Table 4. *In Vitro* ADME Characterization for Selected Compounds

Cpd.	CL h-LM[a] (μL/(min mg) protein)	CL r-LM[b] (μL/(min mg) protein)	CL m-LM[c] (μL/(min mg) protein)	Caco-2 (Papp)[d] (10^{-6} cm/s)	solubility[e] (μg/mL)	cLog *D*[f]
9a	7	123	12	16	6.3−12.5	1.0
9b	7	740	62	32	<1.6	1.4
9h		485	69	44	12.5−25	2.0
19f	35	36	183	35	<1.6	1.5
20e	7	42				1.4
20g	13	78			1.6−3.1	0.47
21	83	636			<3.1	3.8

[a]Intrinsic clearance in human liver microsomes. [b]Intrinsic clearance in rat liver microsomes. [c]Intrinsic clearance in mouse liver microsomes. [d]Caco-2 cell permeability assay. Papp, permeability coefficient in the apical to basolateral direction. [e]Aqueous kinetic solubility measured at pH = 6.5. [f]Calculated Log *D* at pH 7.4 (Chem Axon JChem, version 21.2).

position R^4. The resulting compounds (**19g−i**) were found inactive. This advocates for a deleterious effect associated with a substituent in the *ortho* position (R^4), which might induce a detrimental repulsive conformational change.

Encouraged by the promising result obtained with **19f**, variations of the R^6 substituent were undertaken (**19j−l**) to fine-tune the best possible combinations. Among the substituents evaluated, only a fluorine atom was well accommodated (**19j**, IC_{50} = 54 nM), which indicates possible steric constraints at this position. In addition, alternatives to the ether oxygen atom of the spacer were envisaged. Its replacement by an *N*-methyl or thiol ether resulted in considerable loss of potency (**19m,n**), whereas the sulfone analogue was totally inactive (data not shown). Shifting the acidic function to the *meta* position in the optimal linker gave disappointing activity (**19o**). Lastly, as 4-(methoxymethyl)benzoic acid seemed to be the optimal RHS, it appeared sensible to walk this group through positions R^4, R^5, and R^6. At best, the R^4 position provided antimalarial potency only in the micromolar range.

In total, 4-(methoxymethyl)benzoic acid at position R^3 with R^4 = R^5 = R^6 = H appeared as the optimal RHS. In-depth investigation of the RHS of the molecule shed light on a strongly beneficial modification by positioning the ether oxygen atom at the central position of the three-atom linker between the quinazolinone and the benzoic acid moieties while removing the fluorine at position R^4. SAR data suggest establishment of key interaction(s) through this ether oxygen atom, most likely of the hydrogen bond and/or dipole bond type(s) with a well-defined geometry.

Rudimentary SAR with Potential Optimal Linker. The favorable contribution of 4-(methoxymethyl)benzoic acid as RHS was then combined with LHS substituents previously investigated to check whether the LHS SAR remained similar. The antiplasmodial activities of representative compounds are combined in Table 3. Comparable shifts in potency to that observed with compounds of type **9** were noted when comparing **19f** with unsubstituted benzyl, *meta*-methoxybenzyl, and *para*-ethylbenzyl analogues (compounds **20a−d**). Methylation at the benzylic position remained not tolerated. These findings appeared convincing enough to posit that the LHS SAR was following a similar trend with this new linker. Finally, a few simple changes were envisaged to check whether potential liabilities could be readily solved without recourse to thorough optimization of **19f**. To address potential metabolic stability issues related to the ethyl substituent, its replacement by a trifluoromethyl group was undertaken in **20e**. The bioisosterism of the trifluoromethyl group has been questioned recently with studies arguing for its steric effect being rather similar to an ethyl than isopropyl group.[16−18] In that regard, the observed 16-fold potency loss was somewhat disappointing and suggested that alkyl substituents were favored and/or that tight steric constraints were present around *meta* substitution of the benzyl group. In addition, picolyl analogues of **19f** (compounds **20f−g**) were considered to enhance the aqueous solubility but showed unsatisfactory potencies. Lastly, the primary amide analogue of **19f** was found to be moderately potent (**21**, IC_{50} = 310 nM). This result suggests potential for replacement of the acidic moiety provided the associated potency loss could be compensated. Indeed, the acidic nature of the frontrunner compound **19f** can possibly constitute a concern for its development as an antimalarial due to the expected low volume of distribution. If confirmed, this would pose challenges in terms of achieving the long half-life required for single-dose treatment of malaria[8,19] and would require clearance to be as low as possible. Moreover, acyl glucuronide metabolite formation[20−22] would need be to be investigated to assess whether this could be a concern for further development of this acidic chemotype.

Overall, **19f** appeared as the most potent compound with acceptable ligand efficiency and lipophilic efficiency (0.30 and 5.22, respectively) among those tested.

***In Vitro* ADMET.** **19f** and representative compounds from this chemical class (**9a**, **9b**, **9h**, **20d**, **20e**) were subjected to *in vitro* ADME profiling, with respect to oxidative metabolism in liver microsomes, Caco-2 cell monolayer permeation, and aqueous solubility. Results are combined in Table 4.

9a and **9b** were used as representative compounds of the original chemotype and demonstrated greater stability in human liver microsomes than compounds of types **19−20**. Interestingly, direct comparison of the close structural analogues **9h** and **19f** did not show any obvious detrimental impact associated with the shift of the ether oxygen atom at the central position of the linker, thereby creating two potential metabolic hot spots. This was further confirmed by the good metabolic stability demonstrated by **20e** in human liver microsomes. Despite disappointing antiplasmodial activity, the beneficial impact of the replacement of the ethyl substituent by a trifluoromethyl designates this position as a metabolic soft spot with respect to oxidative metabolism and underlines the possibility of achieving acceptable stability through structural modifications. Moreover, this modification did not change markedly the calculated Log *D* (pH 7.4), which remains in a favorable range (~2.0). Overall, lower Log *D* was associated with improved microsomal stability as exemplified by compounds **20e** and **20g**. It is noteworthy to mention that the acidic moiety appears to have a strongly beneficial impact on Log *D* as illustrated by the comparison between **19f** and its amide analogue **21**, which is likely linked to

https://doi.org/10.1021/acs.jmedchem.1c00441
J. Med. Chem. XXXX, XXX, XXX−XXX

the poor microsomal stability of the latter. On the other hand, microsomal stability was moderate to poor in rat species for all tested compounds, with the best stability obtained with **19f**.

We were encouraged to observe good permeability for this chemical series in spite of the unfavorable polar surface area (PSA), relatively high molecular weight (MW), and the presence of an acidic moiety (e.g., Papp 35 × 10^{-6} cm/s with PSA = 117 Å^2 and MW = 471 g/mol for **19f**). In terms of aqueous solubility, we hoped that the linker harbored by **19f** would be beneficial, when compared to compounds of type **9**, thanks to the two ether oxygen lone pairs readily accessible to form hydrogen bonds with water. On the contrary, results showed a detrimental impact with solubility below 1.6 μg/mL. These data are in line with the higher calculated Log *D* for compounds of type **19** (1.5 and 2.0 for **19f** and **9h**, respectively). Moreover, introduction of an unflanked pyridine nitrogen atom with **20g** resulted only in a marginal improvement of the kinetic solubility within the range of 1.6−3.1 μg/mL at pH 6.5 despite the lower calculated Log *D*. This finding was particularly surprising, and we hypothesized that the poor aqueous solubility might be due to the tight crystal packing related to the high molecular planarity[23] induced by the quinazolinone ring. To confirm this, melting points were measured for compounds **19f** and **20e** (238.5 and 249.5 °C, respectively). These high melting points advocate for more drastic chemical modifications to be performed during optimization of **19f** by targeting disruption of crystal packing.

Table 5 summarizes additional ADMET data gathered on **19f**. First, rat and human hepatocyte stability data were collected.

Table 5. Additional *In Vitro* ADMET Profiling of Compound 19f

CL h-heps[a]	15 μL/min/10^6 cells
CL r-heps[b]	6 μL/min/10^6 cells
h-plasma stability[c]	100%
r-plasma stability[d]	93.4%
h-Fu[e]	0.2%
CYP1A2[f]	<10% @ 10 μM
CYP2C9[f]	55% @ 10 μM
CYP2D6[f]	<10% @ 10 μM
CYP3A4[f]	<10% @ 10 μM
hERG IC_{50}[g]	>30 μM
HEK293 CC_{50}[h]	>40 μM

[a]Intrinsic clearance in human hepatocytes. [b]Intrinsic clearance in rat hepatocytes. [c]Human plasma stability at 37 °C (% remaining after 2 h). [d]Rat plasma stability at 37 °C (% remaining after 2 h). [e]Plasma protein binding assay, rapid equilibrium dialysis. Fu, fraction unbound. [f]Inhibition of cytochrome P450 isoforms. [g]QPatch automated patch clamp. [h]72 h assay, *N* = 4.

Microsome and hepatocyte-predicted hepatic extraction ratios were found to be in the same range (0.5−0.6 and 0.3−0.4 in humans and rats, respectively, without correction for binding). This was reassuring since phase II metabolism could have been a concern for such a molecule harboring an acid function and four benzylic positions. Moreover, **19f** demonstrated good stability in rat and human plasma, removing concerns regarding the possible degradation of the amide moiety by hydrolytic enzymes present in plasma. Plasma protein binding was found to be relatively high (99.8%). No inhibition was noted against CYP450s at 10 μM except for 2C9, which is not surprising due to the acidic nature of the molecule. Finally, **19f** exhibited a low probability to generate QT prolongation and no potential cytotoxicity against mammalian cells based on the lack of inhibition of hERG and HEK293 cellular assays, respectively.

In summary, despite the poor aqueous solubility and poor microsomal stability in mouse, **19f** demonstrated some encouraging *in vitro* ADMET properties with good permeability, moderate metabolic stability in humans and rats, no major CYP inhibition risk, and no risk of hERG.

Inhibition of MMP-1 and MMP-14. Although this chemical series is still at an early stage, the frontrunner was tested against MMP-1 and MMP-14 to assess any potential risks. At 10 μM, **19f** showed 11.3 and 10.8% inhibition of MMP-1 and MMP-14, respectively (*N* = 2). The low level of inhibition observed against these two MMPs is reassuring at this stage but would need to be monitored during the optimization course of this chemical series.

Antimalarial Profile. The efficacy of **19f** was profiled against various life-cycle stages. Beyond the intraerythrocytic stage, the malaria parasite life cycle in the human host involves two additional major stages with the liver and sexual blood stages. *In vitro* testing in a *Pf* liver schizont 96 h assay using primary human hepatocytes[24] led to an IC_{50} of ∼75 nM but with only 50% as E_{max}. Precipitation issues were reported and could be a possible explanation for the observed limited maximum efficacy, as well as metabolism due to moderate stability of **19f** in human hepatocytes. Nevertheless, this liver stage activity appeared to be real, as no toxicity was observed against hepatocytes, suggesting that further investigation by testing more stable and soluble compounds was warranted. In addition, no activity was observed against late-stage gametocytes.[25,26] These results underscore promises for the prophylactic activity but a lack of the transmission-blocking potential.

The *in vitro* killing profile was determined in a parasite reduction ratio (PRR) assay that uses a limiting dilution technique to quantify the number of asexual blood-stage parasites that remain viable after drug treatment.[27] Results are depicted in Figure 2 with comparison to reference antimalarials

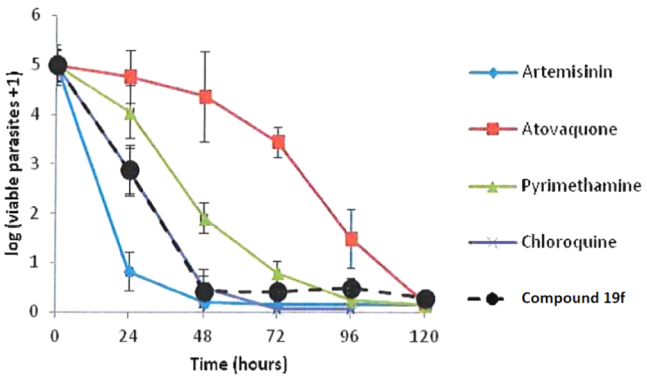

Figure 2. Killing profile of **19f** compared with reference antimalarial drugs (all tested at 10× their respective IC_{50}s).

covering a broad range of killing rates. **19f** benefits from a fast-killing profile similar to chloroquine with a PRR of 4.6 log units over a period of 48 h, a parasite clearance time ($PCT_{99.9\%}$) of 32 h, and no lag phase.

Assessing the risk of resistance at an early stage is critical when developing novel malaria therapeutic agents. In that regard, **19f** was tested against various laboratory-resistant *P. falciparum* strains and was found to potently inhibit growth in all strains tested, irrespective of their geographical origin and resistance

https://doi.org/10.1021/acs.jmedchem.1c00441
J. Med. Chem. XXXX, XXX, XXX−XXX

profile, with respect to the sensitive strain NF54 (Table 6).[28] On the other hand, **19f** showed no cross-resistance when tested against a panel of laboratory strains with mutations in recently identified antimalarial targets from compounds currently in development[6,29] (Table 7).

Table 6. *In Vitro* Intraerythrocytic Antiplasmodial Activity of 19f against Laboratory Strains (Chloroquine and Artesunate as Controls)

laboratory strains	mutated loci	compound 19f IC_{50} (μM)[a]	chloroquine IC_{50} (μM)[a]	artesunate IC_{50} (μM)[a]
NF54[b]		0.060	0.010	0.006
Dd2	*Pf*crt, *Pf*mdr1, *Pf*dhfr, *Pf*dhps	0.033	0.144	0.004
K1	*Pf*crt, *Pf*mdr1, *Pf*dhfr, *Pf*dhps	0.031	0.243	0.003
7G8	*Pf*crt, *Pf*mdr1, *Pf*dhfr, *Pf*dhps	0.016	0.067	0.002
TM90C2b	*Pf*crt, *Pf*mdr1, *Pf*dhfr, *Pf*dhps, Pfcytb$_{Q0}$	0.031	0.160	0.004
Cam3.I	*Pf*crt, *Pf*mdr1, *Pf*dhfr, *Pf*dhps, *Pf*kelch13	0.024	0.126	0.006

[a]72 h [^{3}H]hypoxanthine incorporation assay, mean values from two independent biological replicates; the majority of the individual values varied not more than 10% (maximum 17% for Dd2). [b]sensitive strain.

Table 7. *In Vitro* Antiplasmodial Activity of 19f against Laboratory-Generated Strains

strain generated[a]	mutated locus	mutation references	IC_{50} (μM)[b]
Dd2	wt		0.033
Dd2 DSM265	*Pf*dhodh	30	0.023
Dd2 ELQ-300	*Pf*cytB	31	0.020
Dd2 DDD498	*Pf*eef2	32	0.019
Dd2 KAF156	*Pf*carl	33	0.018
Dd2 MMV048	*Pf*pi4k	34	0.027

[a]Genetically engineered *P. falciparum* strains. Mutations were introduced in the Dd2 wild-type strain. [b]72 h [^{3}H]hypoxanthine incorporation assay, mean values from two independent biological replicates; the majority of the individual values varied not more than 10% (maximum 17% for Dd2 wt); chloroquine and artesunate as controls (mean IC_{50} values of 0.161 and 0.003 μM, respectively).

Overall, the profile of **19f** appears attractive with a fast *in vitro* killing profile, potent activity against resistant strains of malaria, and no cross-resistance against known antimalarials.

***In Vivo* Pharmacokinetics.** On the basis of the *in vitro* DMPK data gathered, we assessed the *in vivo* pharmacokinetic profile of **19f** in rats. Given data previously reported on related chemotypes,[10] **19f** was administered as its sodium salt to enhance the dissolution rate and thereby optimize oral bioavailability. The plasma concentration versus time profiles are shown in Figure 3, and pharmacokinetic parameters are presented in Table 8. The apparent *in vitro* rat whole-blood-to-plasma partitioning ratio of **19f** was determined to be 0.62, indicating limited distribution into erythrocytes, possibly due to the high plasma protein binding.

After intravenous (IV) administration of **19f**, plasma concentration−time profiles exhibited an apparent terminal half-life ($t_{1/2}$) of ∼5 h. *In vivo* blood clearance (plasma CL/blood-to-plasma ratio) was lower than that predicted based on the *in vitro* metabolic stability in rat liver microsomes (15 *vs* 32 mL/(min kg), respectively). This could possibly be explained by not considering the unbound fraction in blood and microsomes in the *in vitro* prediction (rat plasma and microsomal protein binding was not available). Recovery of the unchanged compound in urine was negligible, suggesting that direct urinary excretion was not a major contributor to *in vivo* elimination. The volume of distribution was moderate (blood V_{ss} = 1.4 L/kg). Although this volume of distribution is in a high range for acidic compounds, a very low clearance will be needed to achieve a half-life commensurate with the single-dose cure targeted for treatment of uncomplicated malaria. Therefore, dramatic improvement of the metabolic stability is a major goal for the development of this chemical series for the delivery of an antimalarial preclinical candidate.

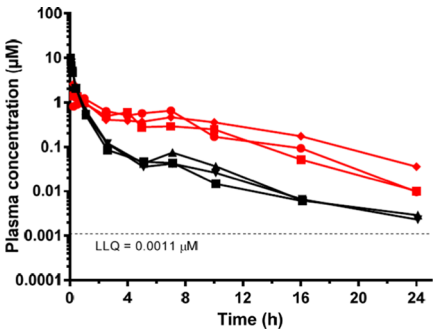

Figure 3. Plasma concentration versus time profiles for **19f** ($Na{\cdot}4H_2O$ salt) in male Sprague Dawley rats (n = 3). IV vehicle: 50% DMA, 50% PEG400; PO vehicle: 0.5% methyl cellulose in water. The black symbols represent the IV profiles and the red, the PO.

Following oral administration (PO), maximum plasma concentrations of **19f** were observed 0.25−1 h post dose and the apparent half-life was comparable to that after IV dosing. The apparent oral bioavailability (F) ranged from 30 to 40%. Given that the *in vivo* blood clearance was equivalent to 20% of the nominal hepatic blood flow in the rat, hepatic first-pass elimination is unlikely to pose a substantial limitation to the oral bioavailability. Rather, oral exposure is likely to be limited by poor absorption due to incomplete dissolution and poor solubility. Indeed, **19f** exhibited very low aqueous solubility at pH 6.5 but good membrane permeability across Caco-2 cells.

A search for potential metabolites of **19f** in plasma and urine samples detected a putative O-dealkylation metabolite (M-120) in pooled urine samples after both intravenous and oral dosing. Based on high-resolution mass measurement and high-collision-energy MS data, this metabolite is likely derived from cleavage of the ether linkage of the methylbenzoic acid moiety. Potential metabolites due to glucuronidation, oxygenation, *N*-dealkylation, and amide hydrolysis were not observed.

Encouraged by this *in vivo* PK profile in rats, we considered an IV PK study in mice. Despite the rather disappointing *in vitro* metabolic stability in this species, further understanding was considered important before testing **19f** in an *in vivo* murine model of malaria. The plasma concentration versus time profiles are reported in Figure 4 and pharmacokinetic parameters in Table 9. The apparent *in vitro* mouse whole-blood-to-plasma partitioning ratio of **19f** was determined to be 0.53. Following IV administration, plasma concentrations remained above the analytical limit of quantitation for the duration of the 24 h sampling period and the apparent terminal half-life was ∼14 h. Assuming that *in vivo* clearance occurs predominantly via

https://doi.org/10.1021/acs.jmedchem.1c00441
J. Med. Chem. XXXX, XXX, XXX−XXX

Table 8. *In Vivo* Pharmacokinetic Profile for Compound 19f ($Na{\cdot}4H_2O$ Salt) in Male Sprague Dawley Rats (n = 3)

route	dose (mg/kg)	$AUC_{0-\infty}$ (h·μM)	F (%)	C_{max} (μM)	t_{max} (h)	$t_{1/2}$ (h)	plasma CL (mL/(min kg))	plasma V_{ss} (L/kg)
IV	1	3.7 ± 0.2				5.3 ± 1.7	9.5 ± 0.6	0.88 ± 0.08
PO	5.6	6.9 ± 1.1	34 ± 5	1.7 ± 0.7	0.5 ± 0.4	3.2 ± 0.9		

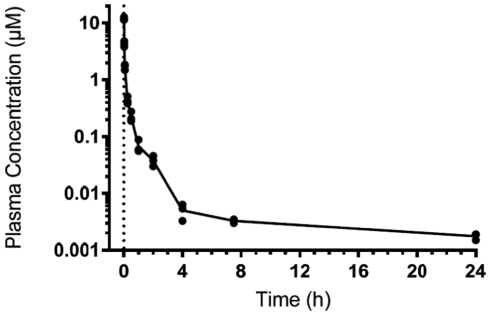

Figure 4. Plasma concentration versus time profiles for **19f** ($Na{\cdot}4H_2O$ salt) in male Swiss outbred mice (n = 3) following IV administration. Vehicle: 5% DMSO in a 0.9% saline base containing 5% solutol HS15.

Table 9. *In Vivo* Pharmacokinetic Profile for Compound 19f ($Na{\cdot}4H_2O$ Salt) in Male Swiss Outbred Mice (n = 3)

route	dose (mg/kg)	$AUC_{0-\infty}$ (h·μM)	plasma CL (mL/(min kg))	blood CL (mL/(min kg))
IV	0.95	1.1	31	57

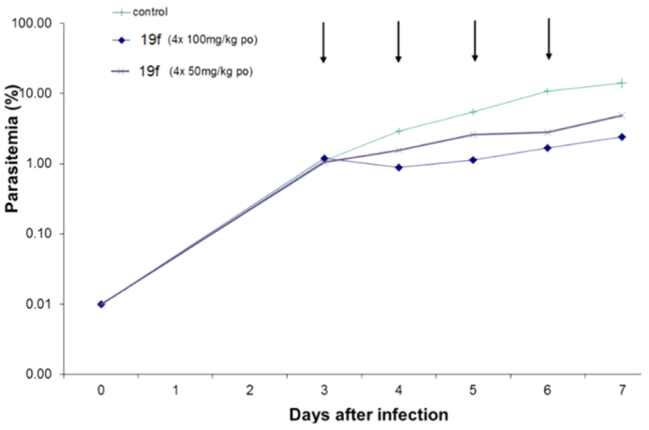

Figure 5. Therapeutic efficacy of **19f** ($Na{\cdot}4H_2O$ salt) in the *in vivo P. falciparum* NODscidIL2Rγnull mouse model of malaria. The arrows indicate the days of oral treatment at 50 and 100 mg/kg in the 4-day test by Peters. Values correspond to the average parasitemia in peripheral blood of n = 2 mice per group.

hepatic elimination, the apparent blood clearance corresponds to approximately 50% of the nominal hepatic blood flow in a mouse (120 mL/(min kg)). This is lower than the predicted blood clearance based on metabolic stability data in mouse liver microsomes (predicted hepatic extraction ratio 0.80). The higher *in vivo* clearance in the mouse compared to the rat confirms interspecies differences in the elimination of this compound in line with microsomal stability data collected *in vitro*.

***In Vivo* Efficacy in a Humanized Murine Model of Malaria.** Due to unfavorable DMPK properties in mice, we tested **19f** at relatively high doses in a *P. falciparum* humanized SCID mouse model[35] with the objective of obtaining proof-of-principle of antimalarial efficacy for this chemical series. The compound was administered as its monosodium tetrahydrate salt orally at 50 and 100 mg/kg over 4 consecutive days. The therapeutic efficacy illustrated in Figure 5 demonstrated that at day 7 post infection, 65 and 83% reductions in activity were measured compared to the untreated control mice at 50 and 100 mg/kg, respectively (n = 2 mice per group). No adverse events were reported. Although the level of efficacy remained modest for such a dose regimen, it was encouraging to see that parasitemia was reduced in a dose-dependent manner despite the suboptimal short exposure exhibited by **19f** in mice (see blood concentration−time profiles on page S12 of the Supporting Information).

CONCLUSIONS

We have identified quinazolinone-2-carboxamide derivatives as novel antimalarial scaffolds. SAR studies led to identification of a double-digit nanomolar inhibitor, **19f**, 95-fold more potent than the original hit compound. Despite suboptimal DMPK and physicochemical properties, **19f** demonstrated oral efficacy in a murine model of human malaria in a dose-dependent manner. The next major goals for this series should focus on improving metabolic stability and aqueous solubility. In that regard, modifications targeting possible metabolic soft spots would benefit from metabolite identification studies, and crystal packing disruption could also be envisaged. Overall, the quinazolinone-2-carboxamide series deserves further investigation to fully assess its potential with respect to the attributes to be demonstrated by novel preclinical candidates for treatment of uncomplicated malaria.

EXPERIMENTAL SECTION

Chemistry. Solvents and chemicals were of reagent grade or better and were obtained from commercial sources. All experiments dealing with moisture-sensitive compounds were conducted under nitrogen. NMR spectra were recorded on Bruker 400 MHz spectrometers. Chemical shifts were referenced with respect to the residual solvent signals (DMSO: 2.50 ppm). Data were reported as follows: chemical shift (δ), integration, multiplicity (br, broad; s, singlet; d, doublet; t, triplet; dd, doublet of doublets; ddd, doublet of doublet of doublets; dt, doublet of triplets; td, triplet of doublets; q, quadruplet; m, multiplet), and coupling constants (J) in hertz. The signal of the amide proton of quinazolinone-2-carboxamide derivatives was reported only when visible (exchange with deuterated solvent prevented its observation in a number of final compounds). Liquid chromatography-mass spectrometry (LC-MS) data provided were obtained using a Shimadzu LC-MS-2020 detector operated in positive or negative electrospray. Analytical HPLC data were obtained using a Shimadzu LC-20AB separation module (Alliance) equipped with a Kinetex EVO C-18 column (3 mm × 2.1 mm, 5 μm). Detection was conducted at 220 nm, 254 nm, and full scan at 210−260 nm with a photodiode array detector. The mobile phase was a linear gradient with a flow rate of 1.5 mL/min using a 95:5 A/B to 5:95 A/B mixture over 1.5 min. Solvent A was 0.0375% TFA in water, and solvent B was 0.01875% TFA in acetonitrile. Silica flash was performed with LCGY-FP0100. For thin-layer chromatography (TLC), alumina sheets from WuXi AppTec coated with silica gel 60 F254 were used. All tested compounds possessed a purity of at least 95% established by HPLC. When the purity of a compound was less than 95%, the percent of purity was specified. Reported yields were not optimized, with emphasis on purity of the product rather than quantity. Melting points were measured with

https://doi.org/10.1021/acs.jmedchem.1c00441
J. Med. Chem. XXXX, XXX, XXX−XXX

CAS-WH-MPA-A instrument (type M70, Mettler Toledo). Amines were purchased from commercial suppliers or synthesized according to literature procedures. Synthesis and characterization of compounds **1**,[10] **2**,[10] **3**,[10] **9c**,[36] **9d**,[36] and **20a**[10] have already been reported in the literature as well as the corresponding synthetic intermediates.[10,36]

General Procedure A for the Synthesis of Compounds of Type 9. *Step 1: Synthesis of tert-Butyl(3,4-difluorophenyl)-carbamate (**5**).* To a solution of compound **4** (17.00 g, 131.67 mmol) in THF (200.00 mL) was added Boc_2O (30.17 g, 138.25 mmol, 31.76 mL). The mixture was stirred at 60 °C for 16 h. TLC (PE/EA = 10:1) indicated disappearance of the starting material and formation of a new spot. The reaction mixture was concentrated under reduced pressure. The residue was diluted with ethyl acetate (100 mL) and washed with saturated citric acid solution (2 × 30 mL) and then saturated with a $NaHCO_3$ solution (30 mL), dried over Na_2SO_4, filtered, and concentrated under reduced pressure. The resulting residue was recrystallized from ethyl acetate/petroleum ether (50 mL/150mL) to give compound **5** as a white solid (28.00 g, 122.15 mmol, 92.8% yield).

*Step 2: Synthesis of 6-((tert-Butoxycarbonyl)amino)-2,3-difluorobenzoic Acid (**6**).* Compound **5** (10.60 g, 46.24 mmol) was degassed and purged with N_2 three times, and then, THF (10.00 mL) was added. The mixture was stirred at −78 °C under a N_2 atmosphere, added dropwise in *s*-BuLi (1.3 M, 78.26 mL), and then stirred at −78 °C for 3 h under a N_2 atmosphere. After that, CO_2 (6.11 g, 138.73 mmol) was added and the resulting reaction mixture was stirred at −78 °C for 1 h under a N_2 atmosphere. TLC (PE/EA = 50:1) indicated disappearance of the starting material and formation of a new spot only. The reaction mixture was quenched by addition of H_2O (20 mL) at −78 °C and stirred at 25 °C for 10 min. The resulting mixture was then washed with *t*-BuOMe (2 × 10 mL). The combined water layers were treated with a 1 M aqueous HCl solution (20 mL) to give a mixture that was extracted with *t*-BuOMe (2 × 40 mL). The combined organic layers were dried over Na_2SO_4, filtered, and concentrated under reduced pressure to give compound **6** as a white solid without further purification (9.00 g, 32.94 mmol, 71.2% yield).

*Step 3: Synthesis of Ethyl 5,6-Difluoro-4-oxo-3,4-dihydroquinazoline-2-carboxylate (**7**).* To a solution of compound **6** (5.00 g, 18.30 mmol) in HCl/dioxane (150.00 mL) was added ethyl cyanoformate (2.15 mL, 2.18 g, 21.96 mmol). The resulting mixture was stirred at 80 °C for 3 h. As LC-MS indicated that compound **6** was consumed completely, the reaction mixture was quenched by addition of a saturated Na_2CO_3 solution (50 mL) at 25 °C, diluted with dichloromethane (50 mL), and extracted with DCM (3 × 100 mL). The combined organic layers were washed with H_2O (2 × 20 mL), dried over Na_2SO_4, filtered, and concentrated under reduced pressure to give compound **7** as a white solid (4.50 g, 17.70 mmol, 96.7% yield). ^{1}H NMR (400 MHz, DMSO-d_6) δ = 12.80 (s, 1H), 8.00−7.95 (m, 1H), 7.71−7.68 (m, 1H), 4.4−4.25 (m, 2H), 1.36−1.27 (m, 3H). LC-MS *m*/*z* 255.2(M + H)$^+$.

*Step 4: Synthesis of Compounds of Type **8**.* At 0 °C under a N_2 atmosphere, $AlMe_3$ (283.61 mg, 3.93 mmol) was added dropwise to a solution of the appropriate amine (1.57 mmol) in toluene (20.0 mL). The resulting mixture was stirred at 0 °C for 30 min; then, compound **7** (200.00 mg, 0.786 mmol) was added at 25 °C for 12 h. LC-MS showed consumption of the starting material and formation of 60% of the desired product. The solvent was removed and the crude mixture was purified by chromatography over silica gel (PE/EA = 1:1) to afford the desired compound **8** in 76−82% yields.

Step 5. At 0 °C under a N_2 atmosphere, the appropriate compound **8** (120.00 mg, 0.350 mmol) and 4-(2-hydroxyethyl)benzoic acid (87.12 mg, 0.524 mmol) were added to a suspension of NaH (60% in mineral oil, 83.88 mg, 2.10 mmol) in DMF (20.0 mL). The resulting mixture was stirred at 25 °C for 1 h and then at 80 °C for 11 h. LC-MS revealed that the starting material was almost consumed and 15% of the desired product was formed. The reaction was quenched with citric acid (50 mL) and extracted with ethyl acetate (3 × 40 mL). The combined organic layers were washed with water (20 mL) and brine (20 mL), dried over Na_2SO_4, and concentrated under reduced pressure. The resulting residue was purified by preparative HPLC (column: Boston Green ODS 150 × 30 mm, 5 μm; mobile phase: water with 0.225% formic acid/CH_3CN, 55/82%; 10 min) to afford the desired compound **9** in 8−17% yields.

Following the above-described general procedure A, using the appropriate amine, compounds **9a**−**l** were obtained with 4−9% overall yields.

*4-(2-((2-(Benzylcarbamoyl)-6-fluoro-4-oxo-3,4-dihydroquinazolin-5-yl)oxy)ethyl)benzoic Acid (**9a**).* ^{1}H NMR (400 MHz, DMSO-d_6) δ 9.53 (t, *J* = 6.0 Hz, 1H), 7.88−7.85 (d, *J* = 8.4 Hz, 2H), 7.79−7.60 (m, 1H), 7.55−7.51 (m, 1H), 7.55−7.42 (m, 2H),7.35 (m, 4H), 7.34 (m, 1H), 4.49−4.47 (d, *J* = 6.4 Hz, 2H), 4.32 (t, *J* = 6.8 Hz, 2H), 4.32 (t, *J* = 6.8 Hz, 2H), 3.17 (t, *J* = 6.8 Hz, 2H). LC-MS *m*/*z* 462.0 (M + H)$^+$.

*4-(2-((2-((Cyclohexylmethyl)carbamoyl)-6-fluoro-4-oxo-3,4-dihydroquinazolin-5-yl)oxy)ethyl)benzoic Acid (**9b**).* ^{1}H NMR (400 MHz, DMSO-d_6) δ 12.02 (br s, 1H), 8.92 (t, *J* = 6.0 Hz, 1H), 7.87 (d, *J* = 8.0 Hz, 2H), 7.78 (t, *J* = 10.0 Hz, 1H), 7.54 (dd, *J* = 4.8, 8.8 Hz, 1H), 7.45 (d, *J* = 8.8 Hz, 2H), 4.32 (t, *J* = 6.8 Hz, 2H), 3.17 (t, *J* = 6.8 Hz, 2H), 3.13 (br t, *J* = 6.8 Hz, 2H), 1.70−1.60 (m, 6H), 1.23−1.012 (m, 3H), 1.01−0.85 (m, 2H). LC-MS *m*/*z* 468.1 (M + H)$^+$.

*4-(2-((2-((3-(Cyclopropylmethoxy)benzyl)carbamoyl)-6-fluoro-4-oxo-3,4-dihydroquinazolin-5-yl)oxy)ethyl)benzoic Acid (**9e**).* ^{1}H NMR (400 MHz, DMSO-d_6) δ 9.48 (br t, *J* = 6.2 Hz, 1H), 7.86 (d, *J* = 8.0 Hz, 2H), 7.78 (t, *J* = 9.7 Hz, 1H), 7.54 (dd, *J* = 4.7, 9.0 Hz, 1H), 7.43 (d, *J* = 8.0 Hz, 2H), 7.22 (t, *J* = 8.0 Hz, 1H), 6.91−6.86 (m, 2H), 6.83−6.78 (m, 1H), 4.44 (br d, *J* = 6.3 Hz, 2H), 4.32 (t, *J* = 6.9 Hz, 1H), 4.36−4.28 (m, 1H), 3.79 (d, *J* = 7.0 Hz, 2H), 3.29−2.87 (m, 2H), 1.27−1.14 (m, 1H), 1.25−1.14 (m, 1H), 0.60−0.52 (m, 2H), 0.35−0.24 (m, 2H). LC-MS *m*/*z* 532.1 (M + H)$^+$.

*4-(2-((6-Fluoro-2-((3-isopropylbenzyl)carbamoyl)-4-oxo-3,4-dihydroquinazolin-5-yl)oxy)ethyl)benzoic Acid (**9f**).* ^{1}H NMR (400 MHz, DMSO-d_6) δ 9.47 (br s, 1H), 8.37 (s, 1H), 7.86 (d, *J* = 8.0 Hz, 2H), 7.77 (br t, *J* = 9.7 Hz, 1H), 7.52 (br dd, *J* = 4.5, 8.8 Hz, 1H), 7.39 (br d, *J* = 7.8 Hz, 2H), 7.27−7.20 (m, 2H), 7.18−7.11 (m, 2H), 4.46 (br d, *J* = 6.3 Hz, 2H), 4.30 (br t, *J* = 6.9 Hz, 2H), 3.16 (br t, *J* = 7.0 Hz, 1H), 2.87 (td, *J* = 6.9, 13.7 Hz, 1H), 1.20 (d, *J* = 6.9 Hz, 6H). LC-MS *m*/*z* 504.3 (M + H)$^+$.

*4-(2-((2-((3-Cyclopropylbenzyl)carbamoyl)-6-fluoro-4-oxo-3,4-dihydroquinazolin-5-yl)oxy)ethyl)benzoic Acid (**9g**).* ^{1}H NMR (400 MHz, DMSO-d_6) δ 9.48 (t, *J* = 6.4 Hz, 1H), 7.94−7.72 (m, 3H), 7.53 (dd, *J* = 4.7, 9.0 Hz, 1H), 7.42 (br d, *J* = 8.3 Hz, 2H), 7.23−7.16 (m, 1H), 7.13−7.06 (m, 2H), 6.94 (d, *J* = 7.6 Hz, 1H), 4.43 (br d, *J* = 6.2 Hz, 2H), 4.31 (t, *J* = 7.0 Hz, 2H), 3.17 (br t, *J* = 6.9 Hz, 2H), 1.94−1.85 (m, 1H), 0.97−0.91 (m, 2H), 0.67−0.61 (m, 2H). LC-MS *m*/*z* 502.1 (M + H)$^+$.

*4-(2-((2-((3-Ethylbenzyl)carbamoyl)-6-fluoro-4-oxo-3,4-dihydroquinazolin-5-yl)oxy)ethyl)benzoic Acid (**9h**).* (92% HPLC purity) ^{1}H NMR (400 MHz, DMSO-d_6) δ 9.50 (t, *J* = 6.0 Hz, 1H), 7.81 (m, 2H), 7.79 (m, 1H), 7.55 (m, 1H), 7.55−7.53 (m, 2H), 7.24−7.09 (m, 4H), 4.33 (d, *J* = 6.4 Hz, 2H), 4.30 (t, *J* = 6.8 Hz, 2H), 3.30 (t, *J* = 6.0 Hz, 2H), 2.56 (m, 2H), 1.24 (m, 3H). LC-MS *m*/*z* 490.1 (M + H)$^+$.

*4-(2-((2-((2-Ethylbenzyl)carbamoyl)-6-fluoro-4-oxo-3,4-dihydroquinazolin-5-yl)oxy)ethyl)benzoic Acid (**9i**).* ^{1}H NMR (400 MHz, DMSO-d_6) δ 8.36 (s, 1H), 7.86 (d, *J* = 8.1 Hz, 2H), 7.78 (t, *J* = 9.7 Hz, 1H), 7.54 (dd, *J* = 4.6, 9.0 Hz, 1H), 7.41 (br d, *J* = 8.1 Hz, 2H), 7.29 (d, *J* = 7.2 Hz, 1H), 7.23−7.12 (m, 3H), 4.51 (br d, *J* = 6.2 Hz, 2H), 4.31 (br t, *J* = 7.0 Hz, 2H), 3.23−3.08 (m, 2H), 2.71 (q, *J* = 7.5 Hz, 2H), 1.19 (t, *J* = 7.5 Hz, 3H). LC-MS *m*/*z* 490.1 (M + H)$^+$.

*4-(2-((2-((4-Ethylbenzyl)carbamoyl)-6-fluoro-4-oxo-3,4-dihydroquinazolin-5-yl)oxy)ethyl)benzoic Acid (**9j**).* (90% HPLC purity). ^{1}H NMR (400 MHz, DMSO-d_6) δ 9.48 (br t, *J* = 6.1 Hz, 1H), 7.86 (br d, *J* = 7.9 Hz, 2H), 7.78 (br t, *J* = 9.7 Hz, 1H), 7.53 (br dd, *J* = 4.5, 9.0 Hz, 1H), 7.44 (br d, *J* = 7.9 Hz, 2H), 4.43 (br d, *J* = 6.1 Hz, 2H), 4.31 (br t, *J* = 6.7 Hz, 2H), 3.17 (br t, *J* = 6.7 Hz, 2H), 2.61−2.55 (m, 2H), 1.15 (br t, *J* = 7.5 Hz, 3H). LC-MS *m*/*z* 490.0 (M + H)$^+$.

*4-(2-((6-Fluoro-4-oxo-2-(phenylcarbamoyl)-3,4-dihydroquinazolin-5-yl)oxy)ethyl)benzoic Acid (**9k**).* ^{1}H NMR (400 MHz, DMSO-d_6) δ 10.63 (s, 1H), 7.90−7.79 (m, 3H), 7.75−7.61 (m, 3H), 7.47 (d, *J* = 8.0 Hz, 2H), 7.31 (t, *J* = 7.8 Hz, 1H), 7.03 (d, *J* = 7.5 Hz, 1H), 4.35 (t, *J* = 6.8 Hz, 2H), 3.20 (br t, *J* = 6.9 Hz, 2H), 2.65−2.60 (m, 2H), 1.21 (t, *J* = 7.6 Hz, 3H). LC-MS *m*/*z* 476.1 (M + H)$^+$.

https://doi.org/10.1021/acs.jmedchem.1c00441
J. Med. Chem. XXXX, XXX, XXX−XXX

4-(2-((2-((1-(3-Ethylphenyl)ethyl)carbamoyl)-6-fluoro-4-oxo-3,4-dihydroquinazolin-5-yl)oxy)ethyl)benzoic Acid (9l). ^{1}H NMR (400 MHz, DMSO-d_6) δ 9.23 (br d, J = 8.4 Hz, 1H), 7.86 (d, J = 8.2 Hz, 2H), 7.78 (t, J = 9.7 Hz, 1H), 7.58 (dd, J = 4.7, 9.0 Hz, 1H), 7.42 (br d, J = 7.9 Hz, 2H), 7.30−7.22 (m, 3H), 7.13−7.07 (m, 1H), 5.10 (m, 1H), 4.31 (t, J = 6.9 Hz, 2H), 3.20−3.12 (m, 1H), 2.64−2.60 (m, 2H), 1.53 (d, J = 7.0 Hz, 3H), 1.18 (t, J = 7.6 Hz, 3H). LC-MS m/z 504.1 $(M + H)^+$.

*4-(2-((2-((3-Ethylbenzyl)(methyl)carbamoyl)-6-fluoro-4-oxo-3,4-dihydroquinazolin-5-yl)oxy)ethyl)benzoic Acid (**9m**).* ^{1}H NMR (400 MHz, DMSO-d_6) δ 7.87 (br d, J = 6.9 Hz, 2H), 7.79−7.70 (m, 1H), 7.49−7.37 (m, 3H), 7.34−7.25 (m, 1H), 7.24−7.10 (m, 3H), 4.62 (br d, J = 12.5 Hz, 2H), 4.40−4.25 (m, 2H), 3.21−3.12 (m, 2H), 2.96−2.84 (m, 3H), 2.68−2.54 (m, 2H), 1.18 (td, J = 7.6, 18.6 Hz, 3H). LC-MS m/z 504.1 $(M + H)^+$.

*5-(4-Carbamoylphenethoxy)-N-(3-ethylbenzyl)-6-fluoro-4-oxo-3,4-dihydroquinazoline-2-carboxamide (**10a**).* To a solution of compound **9h** (50.00 mg, 0.102 mmol) in CH_3CN (2.00 mL) were added DIEA (53.5 μL, 39.60 mg, 0.306 mmol), NH_4Cl (109.28 mg, 2.04 mmol, 71.42 μL), and HATU (77.68 mg, 0.204 mmol) at 25 °C. The resulting mixture was stirred at 25 °C for 12 h. LC-MS showed disappearance of the starting material **9h** and formation of the desired product. The reaction mixture was filtered and concentrated under reduced pressure. The resulting residue was purified by preparative HPLC (column: Boston Green ODS 150 mm × 30 mm, 5 μm; mobile phase: water (0.225% formic acid)/ CH_3CN, 48/72%, 10 min) to afford compound **10a** as a white solid (33.10 mg, 0.064 mmol, 63.0% yield). ^{1}H NMR (400 MHz, DMSO-d_6) δ 9.47−9.45 (t, J = 6.8 Hz, 1H), 8.39 (s, 1H), 7.92−7.81 (m, 2H), 7.79−7.75 (m, 1H), 7.51−7.39 (m, 1H), 7.27−7.22 (m, 2H), 7.17−7.10 (m, 4H), 4.45−4.44 (d, J = 6.4 Hz, 2H), 4.31−4.28 (t, J = 13.6 Hz, 2H), 3.16−3.13 (t, J = 14 Hz, 2H), 2.61−2.55 (m, 2H), 1.18−1.10 (t, J = 7.6 Hz, 3H). LC-MS m/z 489.1 $(M + H)^+$.

*N-(3-Ethylbenzyl)-5-(4-(ethylcarbamoyl)phenethoxy)-6-fluoro-4-oxo-3,4-dihydroquinazoline-2-carboxamide (**10b**).* To a mixture of compound **9h** (30.00 mg, 0.061 mmol) and ethylamine (25.8 mg, 0.613 mmol, 10.0 equiv) in acetonitrile (3.00 mL) were added HATU (116.52 mg, 0.306 mmol) and DIEA (107 μL, 79.21 mg, 0.613 mmol) in one portion at 20 °C, and then, the mixture was stirred at 20 °C for 12 h. LC-MS showed disappearance of the starting material and 15% of the desired product. The solvent was removed to give a residue that was purified by preparative HPLC (column: Phenomenex Synergi C18 Max-RP 250 mm × 50 mm, 10 μm; mobile phase: water (0.1% trifluoracetic acid)/CH_3CN, 44/74%, 12 min) to afford compound **10b** as a white solid. (10.00 mg, 0.019 mmol, 30.6% yield). ^{1}H NMR (400 MHz, DMSO-d_6) δ 12.16 (s, 1H), 9.51 (br t, J = 6.3 Hz, 1H), 8.42 (br t, J = 5.4 Hz, 1H), 7.88−7.72 (m, 3H), 7.54 (dd, J = 4.6, 9.0 Hz, 1H), 7.41 (d, J = 8.0 Hz, 2H), 7.30−7.07 (m, 4H), 4.45 (br d, J = 6.4 Hz, 2H), 4.30 (t, J = 7.0 Hz, 2H), 3.30−3.24 (m, 2H), 3.16 (br t, J = 6.8 Hz, 2H), 2.63−2.57 (m, 2H), 1.26−1.02 (m, 6H). LC-MS m/z 517.2 $(M + H)^+$.

General Procedure B for the Synthesis of Compounds of Type 19. *Step 1, Method A: Esterification to Afford Compounds of Type **12**.* Under a N_2 atmosphere at 25 °C, $SOCl_2$ (6.56 mL, 10.75 g, 90.39 mmol) was added to the appropriate acid of type **11** (30.13 mmol) dissolved in a mixture of DMF/dichloromethane (1.41/100 mL). The reaction mixture was stirred at 50 °C for 2 h. Then, the solvent was removed to give a residue that was added dropwise at 25 °C to a mixture of MeOH (12.22 mL, 9.65 g, 301.30 mmol) and Et_3N (20.88 mL, 15.24 g, 150.65 mmol) in dichloromethane (20 mL). The resulting mixture was stirred at 25 °C for 8 h. TLC (PE/EA = 10:1) showed disappearance of the starting material was consumed and a new main spot with a lower polarity. The reaction was diluted with dichloromethane and quenched with water (200 mL). The organic layer was washed with brine (100 mL), dried over Na_2SO_4, and concentrated under reduced pressure. The resulting residue was purified by chromatography over silica gel (petroleum ether/ethyl acetate = 30:1 to 10: 1) to afford the desired compound of type **12** in 76−86% yields.

*Step 1, Method B: Methylation to Afford Compounds of Type **12**.* Under a N_2 atmosphere, to a mixture of compound of type **11** (13.80 mmol) in acetone (50.00 mL) were added methyl iodide (2.578 mL, 5.877 g, 41.40 mmol) and K_2CO_3 (57.22 g, 414.03 mmol) in one portion at 20 °C. The resulting mixture was stirred at 50 °C for 12 h. TLC (PE/EA = 10:1) showed disappearance of the starting material and formation of a new main spot with a lower polarity. The reaction mixture was filtered, and the filtrate was concentrated under reduced pressure. The residue was dissolved in DCM (500 mL), washed with water (100 mL) and brine (100 mL), dried under Na_2SO_4, and concentrated under reduced pressure to afford compounds of type **12** in 91−96% yields.

*Step 2, Method A: Bromination with DBDMH/BPO to Afford Compounds of Type **13**.* Under a N_2 atmosphere at 20 °C, to a mixture of compound of type **12** (11.74 mmol) in chlorobenzene (100.00 mL) were added 1,3-dibromo-5,5-dimethylhydantoin (DBDMH) (4.03 g, 14.09 mmol) and benzyl peroxide (BPO) (568.76 mg, 2.35 mmol) in one portion. The mixture was stirred at 70 °C for 12 h. TLC (PE/EA = 5:1) showed disappearance of the starting material and a new main spot with a higher polarity. The solvent was removed under reduced pressure. The residue was purified by chromatography over silica gel (PE/EA = 50:1 to 20:1) to afford the desired compound of type **13** in 38−66% yields.

*Step 2, Method B: Bromination with DBDMH/AIBN to Afford Compounds of Type **13**.* Under a N_2 atmosphere, to a mixture of compound **12** (7.173 mmol) in CCl_4 (15 mL) were added AIBN (0.236 g, 1.435 mmol) and DBDMH (2.256 g, 7.890 mmol) in one portion at 25 °C. The resulting mixture was stirred at reflux for 3−12 h. TLC (PE/EA = 10:1) showed disappearance of the starting material and formation of a new main spot with a higher polarity. The reaction mixture was filtered, and the filtrate was concentrated under reduced pressure. The residue was purified by chromatography over silica gel (PE/EA = 20:1 to 10:1) to afford the desired compound of type **13** in 42−68% yields.

*Step 3, Method A: Bromine Displacement to Afford Compounds of Type **15**.* To a solution of compound of type **13** (1.12 mmol) in DMF (10.00 mL) were added K_2CO_3 (309.67 mg, 2.24 mmol) and the appropriate compound of type **14** (1.34 mmol). The mixture was stirred at 25 °C for 3−16 h. LC-MS showed disappearance of the starting material and formation of the desired product. The reaction mixture was quenched by addition of water (20 mL), diluted with EA (20 mL), and extracted with EA (3 × 40 mL). The combined organic layers were washed with H_2O (4 × 15 mL), dried over Na_2SO_4, filtered, and concentrated under reduced pressure. The resulting residue was either purified by silica gel (PE/EA = 20:1 to 3:1) or by preparative HPLC (column: Phenomenex Synergi C18 Max-RP 250x50mm, 10 μm; mobile phase: water (0.225% formic acid)/CH_3CN, 55/80%, 8 min) and washed with saturated $NaHCO_3$ solution to afford the desired compound of type **15** in 66−88% yields.

*Step 3, Method B: Bromine Displacement to Afford Compounds of Type **15**.* To a suspension of NaH (1.04 g, 25.96 mmol, 60% dispersion in mineral oil) in THF (50.00 mL) was added dropwise at 0 °C a mixture of compound **13** (4.33 mmol) and the appropriate compound of type **14** (10.82 mmol) in solution in THF (2 mL). The resulting mixture was stirred at 25 °C for 1−3 h. TLC (PE/EA = 5:1) showed disappearance of the starting material and formation of a new main spot. The reaction mixture was quenched with citric acid (100 mL) and extracted with EA (100 mL). The organic layer was washed with water (20 mL) and brine (20 mL), dried over Na_2SO_4, and concentrated under reduced pressure. The resulting residue was purified by chromatography over silica gel (PE/EA = 30:1 to 1:1) to afford the desired compound of type **15** in 44−67% yields.

*Step 3, Method C: Bromine Displacement to Afford Compounds of Type **15**.* Under N_2 at 20 °C, to a mixture of compound **13** (0.55 g, 2.01 mmol) and the appropriate hydroxymethylbenzoic acid (542.44 mg, 3.01 mmol) in solution in DCM/*n*-hexane (2/8 mL) were added Ag_2O (1.40 g, 6.02 mmol) and 4Å molecular sieves (0.5 g) in one portion. The resulting mixture was stirred at 60 °C for 12 h in complete darkness under a N_2 atmosphere. TLC (PE/EA = 3:1) showed disappearance of the starting material and formation of a new main spot with higher polarity. The reaction mixture was filtered, and the filtrate was concentrated under reduced pressure. The residue was purified by

https://doi.org/10.1021/acs.jmedchem.1c00441
J. Med. Chem. XXXX, XXX, XXX−XXX

chromatography over silica gel (PE/EA = 20:1 to 10:1) to afford compounds of type **15** in 80−89% yields.

*Step 4: Reduction of the Nitro Group to Afford Anilines of Type **16**.* Under a N_2 atmosphere at 20 °C, to a mixture of compound **15** (8.04 mmol) in EtOH (100.00 mL) were added Fe (4.49 g, 80.40 mmol) and NH_4Cl (2.81 mL, 4.30 g, 80.40 mmol) in one portion. The resulting mixture was stirred at 70 °C for 1 h. LC-MS showed disappearance of the starting material was consumed and formation of the desired product (note: 20−30% was the corresponding acid resulting from hydrolysis of the ester moiety). The reaction mixture was filtered, and the filtrate was concentrated under reduced pressure. The residue was dissolved in EA/THF (50/50 mL), washed with water (100 mL) and brine (100 mL), dried over Na_2SO_4, and concentrated under reduced pressure to give a mixture of the desired compound of type **16** and the corresponding acid that was used as such for the next step.

*Step 5, Method A: Saponification with NaOH to Afford Compounds of Type **17**.* To a solution of compound of type **16** (0.562 mmol) in THF (4.00 mL) were added H_2O (4.00 mL), MeOH (4.00 mL), and NaOH (1.97 g, 49.26 mmol). The resulting mixture was stirred at 25 °C for 16 h. LC-MS showed disappearance of the starting material. The reaction mixture was quenched with 3N aqueous HCl (30 mL) and extracted with EA (4 × 40 mL). The combined organic layers were dried over Na_2SO_4, filtered, and concentrated under reduced pressure to afford the desired compound of type **17** in 92−96% yields for steps 4 and 5.

*Step 5, Method B: Saponification with LiOH to Afford Compounds of Type **17**.* To a mixture of compound of type **16** (2.17 mmol) in H_2O (10.00 mL), MeOH (10.00 mL), and THF (10.00 mL) was added LiOH.H_2O (910.53 mg, 21.70 mmol) in one portion at 25 °C. The resulting mixture was stirred at 25 °C for 16−20 h. LC-MS showed disappearance of the starting material and formation of the desired product. The reaction was quenched with citric acid (200 mL) and extracted with EA (3 × 50 mL). The organic layer was washed with water (50 mL) and brine (50 mL), dried over Na_2SO_4, and concentrated under reduced pressure to afford the desired compound of type **17** in 91−96% yields for steps 4 and 5.

*Step 6: Cyclization to Afford Quinazolinones of Type **18**.* To a solution of compound of type **17** (0.396 mmol) in dioxane (20.00 mL) were added HCl/dioxane (4M, 20 mL) and ethyl cyanoformate (116.46 μL, 117.62 mg, 1.19 mmol). The reaction mixture was stirred at 60 °C and followed by LC-MS. After 6−16 h, LC-MS showed disappearance of the starting material and formation of the desired product. The reaction mixture was quenched by addition of H_2O (20 mL) and extracted with EA or DCM (3 × 40 mL). The combined organic layers were dried over Na_2SO_4, filtered, and concentrated under reduced pressure to afford the desired compound of type **18** in 72−86% yields.

*Step 7: Reaction with (3-Ethylphenyl)methanamine to Afford Final Compounds of Type **19**.* To a solution of compound of type **18** (0.250 mmol) in EtOH (10.00 mL) were added Et_3N (1.04 mL, 7.50 mmol) and (3-ethylphenyl)methanamine (101.32 mg, 0.750 mmol). The mixture was stirred at 25 °C for 16 h. LC-MS showed disappearance of the starting material and formation of the desired compound. The reaction mixture was quenched by addition of H_2O (15 mL) and extracted with EA (3 × 40 mL). The combined organic layers were washed with H_2O (3 × 10 mL), dried over Na_2SO_4, filtered, and concentrated under reduced pressure. The resulting residue was purified by preparative HPLC (column: Boston Green ODS 150 mm × 30 mm, 5 μm; mobile phase: water (0.225% formic acid)/CH_3CN, 30/60%, 10 min) to afford the desired final compound of type **19** in 91−96% yields.

Following the above-described general procedure B, using the appropriate compounds and methods, compounds **19a−r** were obtained with 9−30% overall yields.

*2-(4-((2-((3-Ethylbenzyl)carbamoyl)-6-fluoro-4-oxo-3,4-dihydroquinazolin-5-yl)methoxy)phenyl)acetic Acid (**19a**).* **19a** was obtained starting from 3-fluoro-2-methyl-6-nitrobenzoic acid using method A in step 1, method A in step 2, method A in step 3 using methyl 2-(4-hydroxyphenyl)acetate, and method A in step 5. ^{1}H NMR (400 MHz, DMSO-d_6) δ 9.51 (br t, J = 6.4 Hz, 1H), 7.93−7.75 (m, 2H), 7.27−7.10 (m, 6H), 6.94 (d, J = 8.4 Hz, 2H), 5.71 (s, 2H), 4.46 (d, J = 6.4 Hz, 2H), 3.48 (s, 2H), 2.58 (q, J = 7.6 Hz, 2H), 1.17 (t, J = 7.6 Hz, 3H). LC-MS m/z 490.1 $(M + H)^+$.

*4-((2-((3-Ethylbenzyl)carbamoyl)-6-fluoro-4-oxo-3,4-dihydroquinazolin-5-yl)methoxy)benzoic Acid (**19b**).* **19b** (94% HPLC purity) was obtained starting from 3-fluoro-2-methyl-6-nitrobenzoic acid using method A in step 1, method A in step 2, method A in step 3 using methyl 4-hydroxybenzoate, and method A in step 5. ^{1}H NMR (400 MHz, DMSO-d_6) δ 9.49 (br s, 1H), 8.33 (s, 1H), 7.94−7.73 (m, 4H), 7.27−7.21 (m, 1H), 7.20−7.13 (m, 2H), 7.12−7.04 (m, 3H), 5.81 (br s, 2H), 4.46 (br d, J = 6.4 Hz, 2H), 2.58 (q, J = 7.6 Hz, 2H), 1.17 (t, J = 7.6 Hz, 3H). LC-MS m/z 476.1 $(M + H)^+$.

*4-(((2-((3-Ethylbenzyl)carbamoyl)-6-fluoro-4-oxo-3,4-dihydroquinazolin-5-yl)methoxy)methyl)benzoic Acid (**19c**).* **19c** was obtained starting from 3-fluoro-2-methyl-6-nitrobenzoic acid using method A in step 1, method A in step 2, method B in step 3 using ethyl 4-(hydroxymethyl)benzoate, and method B in step 5. ^{1}H NMR (400 MHz, DMSO-d_6) δ 9.51 (br s, 1H), 7.88 (d, J = 8.2 Hz, 2H), 7.85−7.74 (m, 2H), 7.38 (d, J = 8.1 Hz, 2H), 7.28−7.22 (m, 1H), 7.21−7.14 (m, 2H), 7.11 (d, J = 7.3 Hz, 1H), 5.27 (s, 2H), 4.66 (s, 2H), 4.47 (d, J = 6.4 Hz, 2H), 2.63−2.58 (m, 2H), 1.18 (t, J = 7.6 Hz, 3H). LC-MS m/z 490.1 $(M + H)^+$.

*2-(4-((2-((3-Ethylbenzyl)carbamoyl)-4-oxo-3,4-dihydroquinazolin-5-yl)methoxy)phenyl)acetic Acid (**19d**).* **19d** was obtained starting from 2-methyl-6-nitrobenzoic acid using method B in step 1, method B in step 2, method A in step 3 using methyl 2-(4-hydroxyphenyl)acetate, and method A in step 5. ^{1}H NMR (400 MHz, DMSO-d_6) δ 12.32 (br s, 2H), 9.61 (br t, J = 6.2 Hz, 1H), 7.96−7.89 (m, 1H), 7.79 (d, J = 7.8 Hz, 2H), 7.34−7.29 (m, 1H), 7.28−7.21 (m, 4H), 7.17 (d, J = 7.6 Hz, 1H), 7.01 (d, J = 8.6 Hz, 2H), 5.81 (s, 2H), 4.53 (d, J = 6.4 Hz, 2H), 3.56 (s, 2H), 2.69−2.64 (m, 2H), 1.24 (t, J = 7.6 Hz, 3H). LC-MS m/z 472.1 $(M + H)^+$.

*4-((2-((3-Ethylbenzyl)carbamoyl)-4-oxo-3,4-dihydroquinazolin-5-yl)methoxy)benzoic Acid (**19e**).* **19e** was obtained starting from 2-methyl-6-nitrobenzoic acid using method B in step 1, method B in step 2, method A in step 3 using methyl 4-hydroxybenzoate, and method A in step 5. ^{1}H NMR (400 MHz, DMSO-d_6) δ 12.35 (br s, 2H), 9.56 (br t, J = 6.1 Hz, 1H), 7.92 (d, J = 8.7 Hz, 2H), 7.87 (br t, J = 7.8 Hz, 1H), 7.73 (br dd, J = 7.6, 15.3 Hz, 2H), 7.28−7.23 (m, 1H), 7.21 (s, 1H), 7.17 (br d, J = 7.7 Hz, 1H), 7.10 (br d, J = 8.8 Hz, 2H), 7.15−7.05 (m, 1H), 5.84 (s, 2H), 4.48 (br d, J = 6.4 Hz, 2H), 2.63−2.60 (m, 2H), 1.18 (t, J = 7.6 Hz, 3H). LC-MS m/z 458.1 $(M + H)^+$.

*4-(((2-((3-Ethylbenzyl)carbamoyl)-4-oxo-3,4-dihydroquinazolin-5-yl)methoxy)methyl)benzoic Acid (**19f**).* **19f** was obtained starting from 2-methyl-6-nitrobenzoic acid using method B in step 1, method B in step 2, method B in step 3 using ethyl 4-(hydroxymethyl)benzoate, and method B in step 5. Off-white solid. Mp 238.5 °C. ^{1}H NMR (400 MHz, DMSO-d_6) δ 12.92 (br s, 1H), 12.17 (s, 1H), 9.52 (t, J = 6.0 Hz, 1H), 7.96 (d, J = 8.0 Hz, 2H), 7.91−7.80 (m, 2H), 7.70 (d, J = 7.6 Hz, 1H), 7.55 (d, J = 8.0 Hz, 2H), 7.28−7.22 (m, 1H), 7.21−7.14 (m, 2H), 7.11 (br d, J = 7.6 Hz, 1H), 5.24 (s, 2H), 4.80 (s, 2H), 4.46 (d, J = 6.4 Hz, 2H), 2.59 (q, J = 7.6 Hz, 2H), 1.18 (t, J = 7.6 Hz, 3H). LC-MS m/z 472.1 $(M + H)^+$.

*4-(((6-Chloro-2-((3-ethylbenzyl)carbamoyl)-4-oxo-3,4-dihydroquinazolin-5-yl)methoxy)methyl)benzoic Acid (**19g**).* **19g** was obtained starting from 3-chloro-2-methyl-6-nitrobenzoic acid using method A in step 1, method A in step 2, method B in step 3 using ethyl 4-(hydroxymethyl)benzoate, and method B in step 5. ^{1}H NMR (400 MHz, DMSO-d_6) δ 12.88 (br s, 1H), 12.38 (br s, 1H), 9.56 (br t, J = 6.4 Hz, 1H), 7.97 (d, J = 8.8 Hz, 1H), 7.90 (d, J = 8.2 Hz, 2H), 7.77 (d, J = 8.7 Hz, 1H), 7.46 (d, J = 8.2 Hz, 2H), 7.28−7.22 (m, 1H), 7.20 (s, 1H), 7.18−7.14 (m, 1H), 7.11 (d, J = 7.5 Hz, 1H), 5.38 (s, 2H), 4.71 (s, 2H), 4.46 (d, J = 6.4 Hz, 2H), 2.59 (q, J = 7.6 Hz, 2H), 1.17 (t, J = 7.6 Hz, 3H). LC-MS m/z 530.1 $(M + H)^+$.

*4-(((6-Bromo-2-((3-ethylbenzyl)carbamoyl)-4-oxo-3,4-dihydroquinazolin-5-yl)methoxy)methyl)benzoic Acid (**19h**).* **19h** was obtained starting from 3-bromo-2-methyl-6-nitrobenzoic acid using method A in step 1, method A in step 2, method B in step 3 using ethyl 4-(hydroxymethyl)benzoate, and method B in step 5. ^{1}H NMR (400 MHz, DMSO-d_6) δ 9.51 (br s, 1H), 8.08 (d, J = 8.7 Hz, 1H), 7.89 (d, J =

https://doi.org/10.1021/acs.jmedchem.1c00441
J. Med. Chem. XXXX, XXX, XXX−XXX

8.2 Hz, 2H), 7.67 (d, J = 8.7 Hz, 1H), 7.43 (d, J = 7.8 Hz, 2H), 7.29−7.07 (m, 4H), 5.40 (s, 2H), 4.70 (s, 2H), 4.46 (br d, J = 6.4 Hz, 2H), 2.60 (br s, 2H), 1.17 (t, J = 7.6 Hz, 3H). LC-MS m/z 550.2 $(M + H)^+$.

*4-(((2-((3-Ethylbenzyl)carbamoyl)-6-methoxy-4-oxo-3,4-dihydroquinazolin-5-yl)methoxy)methyl)benzoic Acid (**19i**).* **19i** was obtained starting from 3-methoxy-2-methyl-6-nitrobenzoic acid using method A in step 1, method A in step 2, method B in step 3 using ethyl 4-(hydroxymethyl)benzoate, and method B in step 5. ^{1}H NMR (400 MHz, DMSO-d_6) δ 12.89 (br s, 1H), 11.96 (s, 1H), 9.46 (t, J = 6.5 Hz, 1H), 7.89 (d, J = 8.3 Hz, 2H), 7.82 (d, J = 9.0 Hz, 1H), 7.70 (d, J = 9.2 Hz, 1H), 7.43 (d, J = 8.3 Hz, 2H), 7.28−7.22 (m, 1H), 7.20 (s, 1H), 7.18−7.14 (m, 1H), 7.11 (d, J = 7.4 Hz, 1H), 5.27 (s, 2H), 4.65 (s, 2H), 4.46 (d, J = 6.3 Hz, 2H), 3.93 (s, 3H), 2.59 (q, J = 7.6 Hz, 2H), 1.17 (t, J = 7.6 Hz, 3H). LC-MS m/z 502.3 $(M + H)^+$

*4-(((2-((3-Ethylbenzyl)carbamoyl)-8-fluoro-4-oxo-3,4-dihydroquinazolin-5-yl)methoxy)methyl)benzoic Acid (**19j**).* **19j** was obtained starting from 3-fluoro-6-methyl-2-nitrobenzoic acid using method B in step 1, method B in step 2, method B in step 3 using ethyl 4-(hydroxymethyl)benzoate, and method B in step 5. ^{1}H NMR (400 MHz, DMSO-d_6) δ 9.41 (br t, J = 6.3 Hz, 1H), 7.95 (d, J = 8.1 Hz, 2H), 7.79−7.73 (m, 2H), 7.53 (d, J = 8.2 Hz, 2H), 7.28−7.06 (m, 4H), 5.16 (s, 2H), 4.78 (s, 2H), 4.46 (br d, J = 6.4 Hz, 2H), 2.58 (q, J = 7.6 Hz, 2H), 1.16 (t, J = 7.5 Hz, 3H). LC-MS m/z 509.2 $(M + H)^+$.

*4-(((8-Chloro-2-((3-ethylbenzyl)carbamoyl)-4-oxo-3,4-dihydroquinazolin-5-yl)methoxy)methyl)benzoic Acid (**19k**).* **19k** was obtained starting from 3-chloro-6-methyl-2-nitrobenzoic acid using method B in step 1, method B in step 2, method B in step 3 using ethyl 4-(hydroxymethyl)benzoate, and method B in step 5. ^{1}H NMR (400 MHz, DMSO-d_6) δ 12.55 (br s, 1H), 9.24 (t, J = 6.6 Hz, 1H), 8.03 (d, J = 8.3 Hz, 1H), 7.96 (d, J = 8.3 Hz, 2H), 7.79 (d, J = 8.3 Hz, 1H), 7.56 (s, 1H), 7.29−7.24 (m, 1H), 7.22 (s, 1H), 7.18 (d, J = 7.5 Hz, 1H), 7.12 (d, J = 7.8 Hz, 1H), 5.18 (s, 2H), 4.80 (s, 2H), 4.51 (d, J = 6.4 Hz, 2H), 2.60 (q, J = 7.6 Hz, 2H), 1.18 (t, J = 7.6 Hz, 3H). LC-MS m/z 506.2 $(M + H)^+$.

*4-(((2-((3-Ethylbenzyl)carbamoyl)-8-methoxy-4-oxo-3,4-dihydroquinazolin-5-yl)methoxy)methyl)benzoic Acid (**19l**).* **19l** was obtained starting from 3-methoxy-6-methyl-2-nitrobenzoic acid using method B in step 1, method B in step 2, method B in step 3 using ethyl 4-(hydroxymethyl)benzoate, and method B in step 5. ^{1}H NMR (400 MHz, DMSO-d_6) δ 12.22 (br s, 1H), 9.19 (br t, J = 6.3 Hz, 1H), 7.95 (d, J = 8.2 Hz, 2H), 7.73 (d, J = 8.5 Hz, 1H), 7.53 (d, J = 8.2 Hz, 2H), 7.46 (d, J = 8.5 Hz, 1H), 7.28−7.23 (m, 1H), 7.22−7.14 (m, 2H), 7.12 (d, J = 7.5 Hz, 1H), 5.14 (s, 2H), 4.76 (s, 2H), 4.48 (d, J = 6.4 Hz, 2H), 3.93 (s, 3H), 2.63−2.58 (m, 2H), 1.18 (t, J = 7.6 Hz, 3H). LC-MS m/z 502.3 $(M + H)^+$.

*4-((((2-((3-Ethylbenzyl)carbamoyl)-4-oxo-3,4-dihydroquinazolin-5-yl)methyl)(methyl)amino)methyl)benzoic Acid (**19m**).* **19m** was obtained starting from 2-methyl-6-nitrobenzoic acid using method B in step 1, method B in step 2, method A in step 3 using methyl 4-((methylamino)methyl)benzoate, and method A in step 5. ^{1}H NMR: (400 MHz, DMSO-d_6) δ 9.63−9.40 (m, 1H), 8.35 (s, 2H), 7.96−7.79 (m, 4H), 7.67 (dd, J = 1.9, 7.0 Hz, 1H), 7.43 (br d, J = 8.1 Hz, 2H), 7.29−7.08 (m, 4H), 4.46 (br d, J = 6.2 Hz, 2H), 4.27 (s, 2H), 3.69 (br s, 1H), 2.63−2.57 (m, 2H), 2.18 (s, 3H), 1.17 (t, J = 7.6 Hz, 3H). LC-MS m/z 483.3 $(M + H)^+$.

*4-(((2-((3-Ethylbenzyl)carbamoyl)-8-methoxy-4-oxo-3,4-dihydroquinazolin-5-yl)methoxy)methyl)benzoic Acid (**19n**).* **19n** was obtained starting from 2-methyl-6-nitrobenzoic acid using method B in step 1, method B in step 2, method A in step 3 using methyl 4-(mercaptomethyl)benzoate, and method A in step 5. ^{1}H NMR (400 MHz, DMSO-d_6) δ 12.88 (br s, 1H), 12.17 (s, 1H), 9.52 (br t, J = 6.4 Hz, 1H), 7.86 (d, J = 8.2 Hz, 2H), 7.80−7.72 (m, 1H), 7.70−7.64 (m, 1H), 7.45−7.33 (m, 3H), 7.29−7.22 (m, 1H), 7.21−7.14 (m, 2H), 7.11 (br d, J = 7.6 Hz, 1H), 4.47 (d, J = 6.2 Hz, 2H), 4.34 (s, 2H), 3.76 (s, 2H), 2.63−2.58 (m, 2H), 1.18 (t, J = 7.6 Hz, 3H). LC-MS m/z 530.1 $(M + H)^+$.

*3-(((2-((3-Ethylbenzyl)carbamoyl)-4-oxo-3,4-dihydroquinazolin-5-yl)methoxy)methyl)benzoic Acid (**19o**).* **19o** was obtained starting from 2-methyl-6-nitrobenzoic acid using method B in step 1, method B in step 2, method C in step 3 using 3-(hydroxymethyl)benzoic acid, and method B in step 5. ^{1}H NMR (400 MHz, DMSO-d_6) δ 9.53 (br t, J = 6.3 Hz, 1H), 8.00 (s, 1H), 7.94−7.85 (m, 2H), 7.84−7.77 (m, 1H), 7.69 (br t, J = 7.2 Hz, 2H), 7.57−7.48 (m, 1H), 7.28−7.21 (m, 1H), 7.21−7.14 (m, 2H), 7.10 (d, J = 7.5 Hz, 1H), 5.23 (s, 2H), 4.79 (s, 2H), 4.46 (d, J = 6.3 Hz, 2H), 2.59 (q, J = 7.6 Hz, 3H), 1.17 (t, J = 7.6 Hz, 3H). LC-MS m/z 472.2 $(M + H)^+$.

*4-(((2-((3-Ethylbenzyl)carbamoyl)-4-oxo-3,4-dihydroquinazolin-6-yl)methoxy)methyl)benzoic Acid (**19p**).* **19p** was obtained starting from 5-methyl-2-nitrobenzoic acid using method B in step 1, method B in step 2, method C in step 3 using 4-(hydroxymethyl)benzoic acid, and method B in step 5. ^{1}H NMR (400 MHz, DMSO-d_6) δ 12.90 (br s, 1H), 12.28 (br s, 1H), 9.53 (br t, J = 6.2 Hz, 1H), 8.17 (s, 1H), 7.95 (d, J = 8.3 Hz, 2H), 7.91−7.85 (m, 1H), 7.79 (d, J = 8.3 Hz, 1H), 7.81−7.75 (m, 1H), 7.51 (d, J = 8.3 Hz, 2H), 7.28−7.22 (m, 1H), 7.20 (s, 1H), 7.19−7.15 (m, 1H), 7.11 (d, J = 7.3 Hz, 1H), 4.75 (s, 2H), 4.69 (s, 2H), 4.46 (d, J = 6.4 Hz, 2H), 3.30 (br s, 2H), 2.63−2.58 (m, 3H), 1.18 (t, J = 7.6 Hz, 3H). LC-MS m/z 472.1 $(M + H)^+$.

*4-(((2-((3-Ethylbenzyl)carbamoyl)-4-oxo-3,4-dihydroquinazolin-7-yl)methoxy)methyl)benzoic Acid (**19q**).* **19q** was obtained starting from 4-methyl-2-nitrobenzoic acid using method B in step 1, method B in step 2, method C in step 3 using 4-(hydroxymethyl)benzoic acid, and method B in step 5. ^{1}H NMR (400 MHz, DMSO-d_6) δ 12.95 (br s, 1H), 12.28 (s, 1H), 9.55 (t, J = 6.2 Hz, 1H), 8.17 (d, J = 8.2 Hz, 1H), 7.96 (d, J = 8.2 Hz, 2H), 7.77 (s, 1H), 7.60 (d, J = 8.0 Hz, 1H), 7.52 (d, J = 8.4 Hz, 2H), 7.27−7.22 (m, 1H), 7.20 (s, 1H), 7.18−7.14 (m, 1H), 7.11 (d, J = 7.7 Hz, 1H), 4.79 (s, 2H), 4.71 (s, 2H), 4.46 (d, J = 6.3 Hz, 2H), 2.62−2.58 (m, 2H), 1.17 (t, J = 7.6 Hz, 3H). LC-MS m/z 472.1 $(M + H)^+$.

*4-(((2-((3-Ethylbenzyl)carbamoyl)-4-oxo-3,4-dihydroquinazolin-8-yl)methoxy)methyl)benzoic Acid (**19r**).* **19r** was obtained starting from 3-methyl-2-nitrobenzoic acid using method B in step 1, method B in step 2, method C in step 3 using 4-(hydroxymethyl)benzoic acid, and method B in step 5. ^{1}H NMR (400 MHz, DMSO-d_6) δ 9.46 (t, J = 6.4 Hz, 1H), 8.17−8.09 (m, 1H), 7.99 (d, J = 6.5 Hz, 1H), 7.93 (d, J = 8.2 Hz, 2H), 7.63 (t, J = 7.7 Hz, 1H), 7.49 (d, J = 8.2 Hz, 2H), 7.27−7.21 (m, 1H), 7.20 (s, 1H), 7.18−7.14 (m, 1H), 7.11 (d, J = 7.3 Hz, 1H), 5.19 (s, 2H), 4.75 (s, 2H), 4.52 (d, J = 6.4 Hz, 2H), 2.58 (q, J = 7.5 Hz, 2H), 1.16 (t, J = 7.6 Hz, 3H). LC-MS m/z 472.2 $(M + H)^+$.

General Procedure C for the Synthesis of Compounds of Type 20. A mixture of compound **15f** (70 mg, 0.183 mmol), the appropriate amine (0.549 mmol), and Et_3N (127.41 μL, 92.62 mg, 0.915 mmol) in EtOH (5.00 mL) was stirred at 50 °C for 24 h. LC-MS showed disappearance of the starting material and formation of the desired product. The reaction mixture was quenched with HCl (50 mL) and then extracted with EA (3 × 40 mL). The combined organic layers were washed with water (20 mL) and brine (20 mL), dried over Na_2SO_4, and concentrated under reduced pressure. The crude mixture was triturated with CH_3CN (20 mL) to afford the desired compound of type **20**.

Following the above-described general procedure C, using the appropriate compounds and methods, compounds **20b−g** were obtained with 65−80% yields.

*4-(((2-(Benzylcarbamoyl)-4-oxo-3,4-dihydroquinazolin-5-yl)methoxy)methyl)benzoic Acid (**20b**).* ^{1}H NMR (400 MHz, DMSO-d_6) δ 9.56 (br t, J = 5.6 Hz, 1H), 7.95 (d, J = 8.2 Hz, 2H), 7.91−7.79 (m, 2H), 7.70 (d, J = 7.2 Hz, 1H), 7.54 (d, J = 8.3 Hz, 2H), 7.39−7.30 (m, 3H), 7.39−7.30 (m, 1H), 7.29−7.21 (m, 1H), 5.22 (s, 2H), 4.79 (s, 2H), 4.53−4.44 (m, 2H). LC-MS m/z 444.1 $(M + H)^+$.

*4-(((2-((4-Ethylbenzyl)carbamoyl)-4-oxo-3,4-dihydroquinazolin-5-yl)methoxy)methyl)benzoic Acid (**20c**).* ^{1}H NMR (400 MHz, DMSO-d_6) δ 9.52 (br s, 1H), 7.96 (d, J = 8.3 Hz, 2H), 7.91−7.86 (m, 1H), 7.85−7.80 (m, 1H), 7.70 (br d, J = 7.9 Hz, 1H), 7.55 (d, J = 8.2 Hz, 2H), 7.29−7.24 (m, 2H), 7.19−7.15 (m, 2H), 5.23 (s, 2H), 4.80 (s, 2H), 4.44 (d, J = 6.3 Hz, 2H), 2.61−2.55 (m, 2H), 1.16 (t, J = 7.6 Hz, 3H). LC-MS m/z 472.2 $(M + H)^+$.

*4-(((2-((3-Ethylbenzyl)(methyl)carbamoyl)-4-oxo-3,4-dihydroquinazolin-5-yl)methoxy)methyl)benzoic Acid (**20d**).* ^{1}H NMR (400 MHz, DMSO-d_6) δ 9.24 (d, J = 8.4 Hz, 1H), 7.90 (d, J = 8.1 Hz, 2H), 7.85−7.80 (m, 1H), 7.79−7.74 (m, 1H), 7.70 (d, J = 7.8 Hz, 1H), 7.47 (d, J = 8.2 Hz, 2H), 7.24−7.18 (m, 3H), 7.07−7.02 (m, 1H), 5.16 (s,

https://doi.org/10.1021/acs.jmedchem.1c00441
J. Med. Chem. XXXX, XXX, XXX−XXX

2H), 5.12−4.99 (m, 1H), 4.73 (s, 2H), 2.54 (q, J = 7.7 Hz, 2H), 1.49 (d, J = 7.0 Hz, 3H), 1.12 (t, J = 7.6 Hz, 3H). LC-MS m/z 486.2 $(M + H)^+$.

*4-((((4-Oxo-2-((3-(trifluoromethyl)benzyl)carbamoyl)-3,4-dihydroquinazolin-5-yl)methoxy)methyl)benzoic Acid (**20e**).* ^{1}H NMR (400 MHz, DMSO-d_6) δ 12.18 (s, 1H), 9.69 (br t, J = 5.6 Hz, 1H), 7.95 (d, J = 8.0 Hz, 2H), 7.92−7.80 (m, 2H), 7.75−7.57 (m, 5H), 7.55 (br d, J = 8.2 Hz, 2H), 5.23 (s, 2H), 4.80 (s, 2H), 4.56 (br d, J = 6.4 Hz, 2H). LC-MS m/z 512.0 $(M + H)^+$.

*4-(((2-((((4-Ethylpyridin-2-yl)methyl)carbamoyl)-4-oxo-3,4-dihydroquinazolin-5-yl)methoxy)methyl)benzoic Acid (**20f**).* ^{1}H NMR (400 MHz, DMSO-d_6) δ 12.23 (br s, 1H), 9.52 (br s, 1H), 8.43 (br d, J = 5.1 Hz, 1H), 7.96 (br d, J = 7.9 Hz, 2H), 7.92−7.80 (m, 2H), 7.72 (br d, J = 7.9 Hz, 1H), 7.55 (br d, J = 8.1 Hz, 2H), 7.31−7.14 (m, 2H), 5.27−5.20 (m, 2H), 4.80 (s, 2H), 4.58 (br d, J = 6.0 Hz, 2H), 2.63 (br s, 2H), 1.17 (t, J = 7.5 Hz, 3H). LC-MS m/z 473.2 $(M + H)^+$.

*4-(((2-((((5-Ethylpyridin-3-yl)methyl)carbamoyl)-4-oxo-3,4-dihydroquinazolin-5-yl)methoxy)methyl)benzoic Acid (**20g**).* Off-white solid. Mp 249.5 °C. ^{1}H NMR (400 MHz, DMSO-d_6) δ 12.69−11.61 (m, 1H), 9.71 (t, J = 5.9 Hz, 1H), 8.68 (d, J = 7.0 Hz, 2H), 8.29 (s, 1H), 7.95 (d, J = 7.9 Hz, 2H), 7.91−7.78 (m, 2H), 7.70 (d, J = 7.8 Hz, 1H), 7.54 (d, J = 7.8 Hz, 2H), 5.22 (s, 2H), 4.78 (s, 2H), 4.63 (d, J = 6.0 Hz, 2H), 2.77 (q, J = 7.4 Hz, 2H), 1.22 (t, J = 7.5 Hz, 3H). LC-MS m/z 473.3 $(M + H)^+$.

*5-(((4-Carbamoylbenzyl)oxy)methyl)-N-(3-ethylbenzyl)-4-oxo-3,4-dihydroquinazoline-2-carboxamide (**21**).* To a mixture of **19f** (0.06 g, 0.127 mmol) and aqueous solution of NH_4Cl (89 μL, 136.14 mg, 2.55 mmol) in DMF (5 mL) were added EDCI (73.18 mg, 0.382 mmol), HOBt (51.58 mg, 0.382 mmol), and DIEA (221.65 μL, 164.46 mg, 1.27 mmol) in one portion. The mixture was stirred at 25 °C for 12 h. LC-MS showed disappearance of the starting material and formation of the desired product. The reaction mixture was poured into water (20 mL), and the resulting solid was collected by filtration. The solid was triturated with CH_3CN (10 mL × 2) and MTBE (20 mL) to afford compound **21** (16 mg, 0.032 mmol, 25% yield, 94% HPLC purity) as a white solid. ^{1}H NMR (400 MHz, DMSO-d_6) δ 12.0 (br s, 1H), 9.53 (t, J = 1.6 Hz, 2H), 7.97 (br s, 1H), 7.91−7.85 (m, 3H), 7.85−7.80 (m, 1H), 7.70 (br d, J = 7.6 Hz, 1H), 7.50 (d, J = 8.4 Hz, 2H), 7.35 (br s, 1H), 7.27−7.22 (m, 1H), 7.19 (s, 1H), 7.16 (br d, J = 7.6 Hz, 1H), 7.11 (br d, J = 7.6 Hz, 1H), 5.22 (s, 2H), 4.77 (s, 2H), 4.46 (d, J = 6.4 Hz, 2H), 2.61 (q, J = 7.6 Hz, 2H), 1.17 (t, J = 7.6 Hz, 3H). LC-MS m/z 471.3 $(M + H)^+$.

*Preparation of the Sodium Salt of Compound 19f: Sodium 4-(((2-((3-Ethylbenzyl)carbamoyl)-4-oxo-3,4-dihydroquinazolin-5-yl)methoxy)methyl)benzoate Tetrahydrate (**19f** Na·4H$_2$O).* A total of 0.01 M aqueous NaOH (24.93 mL, 0.249 mmol) was added dropwise at 20 °C to compound **19f** (0.115 g, 0.244 mmol) in solution in THF/CH_3OH (20/20 mL). The resulting mixture was stirred at 20 °C for 1 h. The organic solvents were then removed under reduced pressure, and methanol (10 mL) was added to the residual suspension. The resulting suspension was stirred at room temperature for 30 min and cooled to 10 °C. The precipitated solid was collected and washed with cold methanol to afford the desired sodium salt as a white solid. Elemental analysis was consistent with a monosodium tetrahydrate salt (0.118 g, 0.209 mmol, 86% yield). ^{1}H NMR (400 MHz, DMSO-d_6) δ 9.47 (br t, J = 6.1 Hz, 1H), 7.93 (d, J = 7.9 Hz, 2H), 7.86−7.76 (m, 2H), 7.69 (d, J = 8.1 Hz, 1H), 7.41 (d, J = 8.1 Hz, 2H), 7.33−7.27 (m, 1H), 7.26−7.19 (m, 2H), 7.16 (d, J = 7.5 Hz, 1H), 5.29 (s, 2H), 4.77 (s, 2H), 4.51 (d, J = 6.1 Hz, 2H), 2.65 (q, J = 7.6 Hz, 2H), 1.23 (t, J = 7.6 Hz, 3H). LC-MS m/z 472.3 $(M + H)^+$. Elemental analysis calculated for $C_{27}H_{24}N_3O_5Na\cdot 4H_2O$: C, 57.34; H, 5.70; N, 7.43; O: 25.46; Na, 4.07. Found: C, 57.37; H, 5.55; N, 7.29; Na, 4.22.

BIOLOGICAL ASSAYS

Intraerythrocytic *Pf* 3D7 and Dd2 Inhibition Growth Assay. It utilizes the DNA-intercalating dye 4′,6′,-diamidino-2-phenylindole (DAPI) to monitor changes in the parasite number observed within infected erythrocytes. This assay was performed as previously reported.[9] In brief, *Pf* parasites (3D7 and Dd2 strains) were cultured in RPMI1640 media supplemented with hypoxanthine, HEPES, 2.5 mg/mL AlbuMAX II, and 5% human serum. Compounds were incubated in the presence of 2% sorbitol synchronized ring-stage parasites in a total assay volume of 50 μL, for 72 h at 37 °C and 5% CO_2, 5% O_2 in poly-D-lysine-coated imaging plates. After incubation, the plates were stained with DAPI in the presence of saponin and Triton X-100 and incubated for a further 8 h at room temperature in the dark before imaging using the Opera (PerkinElmer). The digital images obtained from each well were analyzed using spot detection software. Pyrimethamine, chloroquine, artesunate, DHA, and puromycin were used as internal controls in all experiments.

HEK293 Alamar Blue Viability Estimation Assay. It was performed as previously reported.[15] Incubation times, compound additions, and plate read were as per the Pf 3D7 growth assay, with the exception that Alamar Blue was diluted in HEK293 growth media before addition, and incubation of Alamar Blue at 37 °C, in 5% CO_2, was for 4 h, followed by incubation at room temperature for 20 h. Puromycin (Calbiochem) was used as the control.

***In Vitro* Antimalarial Activity against *Pf* Liver Schizonts.** It was performed as previously reported.[24] In brief, primary human hepatocytes were cultured for 2 days and then overlaid with *P. falciparum* NF54 sporozoites and compounds. The supernatant was refreshed daily with fresh compounds. Four days post infection, hepatocytes are immunostained for the presence of Hsp70-positive liver stage parasites.

***Pf* Late-Stage Gametocyte Assay.** It was run as previously described.[25,26] In brief, NF54-pfs16-LUC-GFP parasites were cultured in RPMI1640 media supplemented with hypoxanthine, HEPES, 2.5 mg/ml AlbuMAX II, 5% human serum, and blasticidin for selection. The parasites were processed through a synchronous single cycle of "stress" to induce gametocytogenesis. Under *N*-acetyl-glucosamine (NAG) treatment, asexual parasites were removed, and resultant stage IV gametocytes were isolated using VarioMACS separator columns, adjusted to 10% gametocytsaemia and added to poly-D-lysine-coated imaging plates containing the compounds of interest. After 72 h incubation at 37 °C and 5% CO_2, 5% O_2, MitoTracker Red CM-H2Xros was added to all wells and the plates were incubated for a further 16 h and imaged using an Opera High Content Imaging System to identify elongated gametocytes with demonstrated mitochondrial viability. The percent inhibition of gametocyte inhibition was calculated using 0.4% DMSO (0% inhibition) and 5 μM Puromycin (100% inhibition) to normalize all of the activity data.

Parasite Reduction Ratio Assay. The assay used the limiting dilution technique to quantify the number of parasites remaining viable after drug treatment following a method published previously.[27] *P. falciparum* strain 3D7A (MR4) was treated with compound **19f** at a concentration corresponding to 10x IC_{50}. Conditions of parasites exposed to treatment are identical to the ones used in the IC_{50} determination (2% hematocrit, 0.5% parasitemia). Parasites were exposed to the drug for 120 h, with the drug being renewed daily over the entire treatment period. Samples of parasites were taken from the treated culture every 24 h (24, 48, 72, 96, and 120 h time points), the drug was washed out, and drug-free parasites were cultured in 96-well plates by adding fresh erythrocytes and new culture media. To quantify the number of viable parasites after treatment, 3-fold serial dilutions were used for samples after removing the drug. Parasites were cultured in 96-well microtiter plates to allow all wells with viable parasites to render detectable

https://doi.org/10.1021/acs.jmedchem.1c00441
J. Med. Chem. XXXX, XXX, XXX−XXX

parasitemia. Four independent serial dilutions were performed with each sample to correct for experimental variation. After 21 days of culturing, samples were taken to examine growth. Additional sampling was done after 28 days to confirm growth/no growth. The number of viable parasites was determined by counting the number of wells with growth. Chloroquine, pyrimethamine, atovaquone, and artesunate were used as controls. The following reagent was obtained through BEI Resources, NIAID, NIH: *P. falciparum*, Strain 3D7A, MRA-151, contributed by David Walliker. The human biological samples were sourced ethically, and their research use was in accord with the terms of the informed consents under an IRB/EC-approved protocol.

***Pf*-Resistant Laboratory Strains and Cross-Resistance.** The testing was performed with the modified [^{3}H]-hypoxanthine incorporation assay, as previously reported.[28]

***In Vitro* Metabolism.** Metabolic stability was assessed by incubating test compounds (at a concentration of 0.25 or 0.5 μM) with human, rat, and mouse liver microsomes at 37 °C and 0.4 mg/mL microsomal protein supplemented with an NADPH-regenerating buffer system as described recently.[37] The hepatocyte stability assay was performed by incubating **19f** (0.25 μM) with human or rat cryopreserved hepatocytes suspended in Krebs−Henseleit buffer at 37 °C (1×10^6 cells/mL). Microsome and hepatocyte samples were quenched with the addition of acetonitrile containing diazepam as the internal standard.

Following protein precipitation, samples were centrifuged and the supernatant was removed for quantitative analysis by LC-MS. The *in vitro* CL_{int} values were calculated from the first-order degradation rate constant.

Sample analysis was conducted using a Waters Xevo G2 QTOF mass spectrometer coupled to a Waters Acquity UPLC system. The column was a Supelco Ascentis Express C8 column (50 mm × 2.1 mm, 2.7 μm), and the mobile phase was a water/acetonitrile (each containing 0.05% formic acid) gradient delivered with a 4 min cycle time. The flow rate was 0.4 mL/min, and the injection volume was 5 μL. Detection was conducted via positive electrospray ionization in the multiple reaction monitoring mode with a cone voltage of 30 V. Samples were quantified by comparison to the response for spiked calibration standards prepared in a prequenched blank matrix and analyzed along with the samples.

Stability in Rat and Human Plasma. Human blood was procured from the Australian Red Cross Blood Service. Rat blood was obtained from male Sprague Dawley rats procured from the Animal Resources Centre (Perth). Plasma from each species was separated and pooled (n = 3 donors for human; multiple animals for rat) and stored frozen at −80 °C. On the day of the experiment, plasma was thawed, spiked with DMSO/acetonitrile/water solutions of **19f** to a nominal compound concentration of 1000 ng/mL (maximum final DMSO and acetonitrile concentrations of 0.2% (v/v) and 0.4% (v/v), respectively), and vortexed to mix. Spiked plasma was maintained at 37 °C for 4 h with aliquots taken at various time points and snap-frozen in dry ice. Concentrations of **19f** were quantified by LC-MS relative to calibration standards prepared in blank human or rat plasma, using diazepam as the internal standard and acetonitrile to precipitate plasma proteins. The percentage of test compound remaining in the plasma at each time point was calculated relative to samples taken at 5 min.

Cytochrome P450 Inhibition. Inhibition of cytochrome P450 (CYP) enzymes 1A2, 2C9, 2D6, and 3A4 was conducted utilizing a substrate-specific interaction approach in human liver microsomes as recently described[37] with the exception that the test compound and reference inhibitors were included at only two assay concentrations (1 and 10 μM for **19f** and furafylline (CYP1A2 reference inhibitor), 0.2 and 2 μM for sulfaphenazole (CYP2C9 reference inhibitor), 0.0075 and 0.075 μM for quinidine (CYP2D6 reference inhibitor), and 0.01 and 0.1 μM for ketoconazole (CYP3A4 reference inhibitor)). Concentrations of the substrate-specific metabolites in acetonitrile-quenched samples were determined by UPLC-MS relative to calibration standards prepared in a quenched microsomal matrix. The percent reduction (% inhibition) in the extent of formation of the specific metabolite was assessed at each assay concentration relative to the incubation in the absence of the inhibitor.

Caco-2 Permeability. Apical-to-basolateral (A−B) permeability across Caco-2 cell monolayers was assessed according to methods recently described[37] using an aqueous transport buffer (pH 7.4 Hanks balanced salt solution containing 20 mM HEPES) in both the apical and basolateral chambers. Donor solutions were prepared by spiking a DMSO stock solution of **19f** into transport buffer at a nominal concentration of 20 μM (final DMSO concentration in the donor solution was 0.1% v/v), and the compound flux was assessed over a period of 120 minutes. Concentrations of **19f** were quantified in acceptor and donor chamber samples by LC-MS and mass balance, and apparent permeability (Papp) was calculated as previously described.

Kinetic Solubility Estimation Using Nephelometry. Test compounds in DMSO were spiked into either pH 6.5 phosphate buffer or 0.01 M HCl (approx pH 2.0) with the final DMSO concentration being 1%. After 30 minutes had elapsed, samples were then analyzed via Nephelometry to determine a solubility range.[38] A pH of 6.5 was used to represent the pH of the fasted-state upper small intestine as previously reported.[39]

hERG Assay. The test compound was tested using the QPatch automated patch clamp system (Sophion, Denmark) at four concentrations (using 0.5-log unit dilutions) from a top concentration of 30 μM, against a minimum of two separate cells. Each four-point concentration−response curve was constructed using cumulative double sample additions of each concentration to the same cell. Verapamil was used as the reference positive control compound.

Whole-Blood-to-Plasma Ratio. The compound was spiked to a nominal concentration of 1000 ng/mL, into fresh heparinized whole blood collected from male Sprague Dawley rats approximately 30 min prior to compound spiking and maintained at 37 °C. Aliquots of the spiked whole blood were transferred into fresh microcentrifuge tubes and maintained at 37 °C under a 5% CO_2 atmosphere to maintain a stable pH. At 30 min, aliquots of whole blood were collected, the remaining whole blood was centrifuged for 3 min, and aliquots of the plasma fraction were collected for assessment of the whole-blood-to-plasma partitioning ratio. The whole blood and plasma fraction samples were diluted with an equal volume of the opposite blank matrix (such that both contained a 1:1 ratio of blood/plasma) and immediately snap-frozen in dry ice. All samples were stored frozen at −80 °C until analysis by LC-MS against standards prepared in the same 1:1 blood/plasma matrix. The apparent whole-blood-to-plasma partitioning ratio was calculated as the ratio of the concentration of compound in blood to that in the plasma fraction of the whole blood sample.

https://doi.org/10.1021/acs.jmedchem.1c00441
J. Med. Chem. XXXX, XXX, XXX−XXX

***In Vivo* Pharmacokinetic (PK) Studies.** Studies in rats and mice were conducted using established procedures in accordance with the Australian Code of Practice for the Care and Use of Animals for Scientific Purposes, and study protocols were reviewed and approved by the Monash Institute of Pharmaceutical Sciences Animal Ethics Committee.

Rat PK studies were carried out using six overnight-fasted male Sprague Dawley rats weighing 273−290 g. Rats had access to water ad libitum throughout the pre- and postdose sampling period, and access to food was reinstated 4 h post dose.

The IV dose was administered as a 6 min constant-rate infusion via an indwelling jugular vein cannula in vehicle containing 50% (v/v) DMA/50% (v/v) PEG400 (0.3 mL dose volume), which had been filtered through a 0.22 μm syringe-tip filter prior to dosing. The average measured concentration of **19f** in aliquots of the filtered solution was 1.0 mg/mL. The oral dose was administered by gavage (5 mL/kg dose volume) as a suspension in 0.5% (w/v) methyl cellulose in water. The average measured concentration of **19f** in aliquots of suspension formulation was 1.1 mg/mL. All animals were dosed within 0.5 h of formulation preparation.

Samples of arterial blood and total urine were collected over 24 h post dose. Blood was collected directly into borosilicate vials (at 4 °C) containing heparin, Complete (a protease inhibitor cocktail), and potassium fluoride to minimize the potential for *ex vivo* degradation. Once collected, blood samples were centrifuged, and supernatant plasma was transferred to fresh tubes and stored frozen (−80 °C) until analysis by LC-MS.

The mouse IV PK study was conducted in three male Swiss outbred mice (25−34 g). Mice had access to food and water throughout the pre- and postdose sampling period. The IV dose was administered as a bolus injection into the lateral tail vein (2 mL/kg dose volume) in a solution of 5% DMSO in a base vehicle of 5% (w/v) Solutol HS-15 in 0.9% (w/v) saline solution, which was filtered through a 0.22 μm syringe-tip filter prior to dosing. The average measured concentration of **19f** in aliquots of the filtered solution was 0.48 mg/mL.

Blood was collected via either submandibular bleed or cardiac puncture while mice were under gaseous isoflurane anesthesia, into tubes containing heparin, Complete, and potassium fluoride. A maximum of two samples was taken from each mouse, and three samples were collected at each time point. Blood was separated by centrifugation, and the plasma fraction was analyzed by LC-MS.

LC-MS analysis of **19f** in biological samples (plasma, urine, or mixed matrix samples) was conducted using a Waters Xevo TQ mass spectrometer coupled to a Waters Acquity UPLC system. The column was a Supelco Ascentis Express amide column (50 × 2.1 mm, 2.7 μm), and the mobile phase was a water/acetonitrile (each containing 0.05% formic acid) gradient delivered with a 4 min cycle time. The flow rate was 0.4 mL/min, and the injection volume was 3 μL. Detection was conducted via positive electrospray ionization in multiple reaction monitoring mode monitoring the transition 472.15 > 320.19 m/z. The cone and CID voltages were 35V and 15 V, respectively. Samples were quantified by comparison to the response for spiked calibration standards prepared in the same matrix and analyzed along with the study samples.

A preliminary search for metabolites in selected plasma and urine samples from the *in vivo* rat PK study was performed using high-resolution mass spectrometry operating in the MS^E mode. Metabolite identification was aided using a software-assisted metabolite discovery module of the Waters UNIFI operating system (UNIFI v1.8.0.0).

Plasma concentration vs time profiles from individual animals (for rats) or for the mean at each sample time (mice) were analyzed using noncompartmental methods (PKSolver Version 2.0).

***In Vivo* SCID Mouse Model.** The animal experiments adhered to local and national regulations of laboratory animal welfare in Switzerland (awarded permission no. 2303). Protocols are regularly reviewed and revised following approval by the local authority (Veterinäramt Basel Stadt). Studies were performed following a protocol published previously[35] using the *Pf* 3D70087/N9 strain. Mice were infected intravenously with 2 × 107 *Pf*-infected erythrocytes on day 0. The test compound **19f** (Na·4H_2O salt) was solubilized (suspended) in a solution consisting of 70% Tween-80 (d = 1.08 g/mL) and 30% ethanol (d = 0.81 g/mL), followed by a 10-fold dilution in H_2O. Experimental mice (NODscidIL2Rγnull female) were treated orally at days 3, 4, 5, and 6 post infection with the test compound **19f** (Na·4H_2O salt) at two different doses (50 and 100 mg/kg) and compared to an infected control group for parasitemia reduction on day 7. In total, six animals were used (n = 2 mice per group). Peripheral blood samples (20 μL) were taken at different time points, mixed with 20 μL of H_2O MilliQ, immediately frozen on dry ice, and stored at −80 °C until analysis. Blood samples were analyzed by LC-MS/MS for quantification to determine pharmacokinetic parameters.

MMP-1 Human Matrix Metallopeptidase Enzymatic Assay. The test compound **19f** (tested at 10 μM), reference compound, or water (control) was added to a buffer containing 50 mM Hepes (pH 7.0), 10 mM $CaCl_2$, 0.05% Brij35, and 20 U MMP-1. The fluorescence intensity was then measured at λ_{ex} = 340 nm and λ_{em} = 460 nm using a microplate reader (Envision, Perkin Elmer). This measurement at t = 0 allows the detection of any compound interference with the fluorimetric detection method at these wavelengths. Thereafter, the reaction was initiated by adding 10 μM of the substrate DNP-Pro-Cha-Gly-Cys(Me)-His-Ala-Lys(n-Me-Abz)-NH2 and the mixture was incubated for 20 min at 37 °C. After incubation, the fluorescence intensity emitted by the reaction product Cys(Me)-His-Ala-Lys(n-Me-Abz)-NH2 was measured at the same wavelengths (t = 40). The enzyme activity was determined by subtracting the signal measured at t = 0 from that measured at t = 40. The results are expressed as a percent inhibition of the control activity. The standard inhibitory compound is GM6001, which is tested in each experiment at several concentrations to obtain an inhibition curve from which its IC_{50} value is calculated.

MMP-14 Human Matrix Metallopeptidase Enzymatic Assay. The test compound **19f** (tested at 10 μM), reference compound, or water (control) are mixed with 4 ng of MMP-14 in a buffer containing 50 mM Tris−HCl (pH 7.5) and 10 mM $CaCl_2$. The fluorescence intensity was then measured at λ_{ex} = 340 nm and λ_{em} = 405 nm using a microplate reader (Envision, Perkin Elmer). This measurement at t = 0 allows the detection of any compound interference with the fluorimetric detection method at these wavelengths. Thereafter, the reaction was initiated by adding 2 μM of the substrate Mca-Pro-Leu-Ala-Cys(p-OmeBz)-Trp-Ala-Arg(Dpa)-NH2 and the mixture was incubated for 60 min at 22 °C. After incubation, the fluorescence intensity emitted by the reaction product Mca-Pro-Leu-Ala was measured at the same wavelengths (t = 15). The enzyme activity was determined by subtracting the signal measured at t = 0 from that measured at t = 15. The results are expressed as a percent

https://doi.org/10.1021/acs.jmedchem.1c00441
J. Med. Chem. XXXX, XXX, XXX−XXX

inhibition of the control activity. The standard inhibitory compound is GM6001, which is tested in each experiment at several concentrations to obtain an inhibition curve from which its IC_{50} value is calculated.

■ ASSOCIATED CONTENT

Supporting Information

The Supporting Information is available free of charge at https://pubs.acs.org/doi/10.1021/acs.jmedchem.1c00441.

^{1}H NMR and LC-MS data for compounds **9a**, **9h**, **19f**, and **20e**; *Pf* liver dose−response curve for compound **19f**; and blood concentration−time profile of compound **19f** in SCID mice (PDF)

Molecular formula strings (CSV)

■ AUTHOR INFORMATION

Corresponding Author

Benoît Laleu − *Medicines for Malaria Venture, ICC, 1215 Geneva, Switzerland;* orcid.org/0000-0002-7530-2113; Email: laleub@mmv.org

Authors

Yuichiro Akao − *Takeda Pharmaceutical Company Limited, Fujisawa, Kanagawa 251-8555, Japan*

Atsuko Ochida − *Takeda Pharmaceutical Company Limited, Fujisawa, Kanagawa 251-8555, Japan*

Sandra Duffy − *Discovery Biology, Griffith University, Nathan 4111 Queensland, Australia*

Leonardo Lucantoni − *Discovery Biology, Griffith University, Nathan 4111 Queensland, Australia;* orcid.org/0000-0002-7246-0677

David M. Shackleford − *Centre for Drug Candidate Optimisation, Monash Institute of Pharmaceutical Sciences, Monash University, Parkville, Victoria 3052, Australia*

Gong Chen − *Centre for Drug Candidate Optimisation, Monash Institute of Pharmaceutical Sciences, Monash University, Parkville, Victoria 3052, Australia*

Kasiram Katneni − *Centre for Drug Candidate Optimisation, Monash Institute of Pharmaceutical Sciences, Monash University, Parkville, Victoria 3052, Australia*

Francis C. K. Chiu − *Centre for Drug Candidate Optimisation, Monash Institute of Pharmaceutical Sciences, Monash University, Parkville, Victoria 3052, Australia*

Karen L. White − *Centre for Drug Candidate Optimisation, Monash Institute of Pharmaceutical Sciences, Monash University, Parkville, Victoria 3052, Australia*

Xue Chen − *WuXi AppTec (Wuhan) Company Ltd., Wuhan 430075, China*

Angelika Sturm − *TropIQ Health Sciences, 6534 AT Nijmegen, The Netherlands*

Koen J. Dechering − *TropIQ Health Sciences, 6534 AT Nijmegen, The Netherlands*

Benigno Crespo − *Global Health, GlaxoSmithKline R&D, Tres Cantos 28760 Madrid, Spain*

Laura M. Sanz − *Global Health, GlaxoSmithKline R&D, Tres Cantos 28760 Madrid, Spain;* orcid.org/0000-0003-0796-5211

Binglin Wang − *WuXi AppTec (Wuhan) Company Ltd., Wuhan 430075, China*

Sergio Wittlin − *Swiss Tropical and Public Health Institute, 4002 Basel, Switzerland; University of Basel, 4002 Basel, Switzerland*

Susan A. Charman − *Centre for Drug Candidate Optimisation, Monash Institute of Pharmaceutical Sciences, Monash University, Parkville, Victoria 3052, Australia;* orcid.org/0000-0003-1753-8213

Vicky M. Avery − *Discovery Biology, Griffith University, Nathan 4111 Queensland, Australia*

Nobuo Cho − *Takeda Pharmaceutical Company Limited, Fujisawa, Kanagawa 251-8555, Japan*

Masahiro Kamaura − *Takeda Pharmaceutical Company Limited, Fujisawa, Kanagawa 251-8555, Japan*

Complete contact information is available at: https://pubs.acs.org/10.1021/acs.jmedchem.1c00441

Author Contributions

B.L.: project leader, compound design, writing, original draft; M.K., N.C.: compound design; B.L., M.K., N.C.: conceptualization; S.A.C., V.M.A.: supervisors at CDCO and Griffith, respectively; M.K., N.C., Y.A., A.O., K.L.W., S.D., L.L.: project team; V.M.A., S.D., L.L.: 3D7, Dd2, LSG, and HEK assays; S.A.C., D.M.S., G.C., K.K., F.C.K.C., K.L.W.: DMPK.; X.C., B.W.: chemistry; A.S., K.J.D.: *Pf* liver; B.C., L.M.S.: P.R.R.; S.W.: cross-resistance and SCID. Edits and contributions are from all authors who read and approved the final manuscript.

Funding

Research reported in this publication was supported by the Global Health Innovative Technology (GHIT) Fund under the project title "New Hit-to-Lead Activity for New Anti-malarials between MMV and Takeda" (Project ID: H2016−205)

Notes

The authors declare the following competing financial interest(s): The authors declare the following financial interest(s): BL is a MMV employee; YA, AO are Takeda employees; BC, LMS are GSK employees.

■ ACKNOWLEDGMENTS

The authors wish to thank the Australian Red Cross Blood Service for the provision of human red blood cells in accordance with agreement 19-05QLD-21. Dr. Mitsuyuki Shimada and Dr. Brice Campo are thanked for facilitating project transfer from Takeda to MMV.

■ ABBREVIATIONS USED

ADME, absorption-distribution-metabolism-excretion; ADMET, absorption-distribution-metabolism-excretion-toxicity; CL, clearance; DHA, dihydroartemisinin; DIPEA, *N*,*N*-diisopropylethylamine; DMPK, drug metabolism pharmacokinetics; EA, ethyl acetate; Fu, fraction unbound; F, bioavailability; hERG, human ether-à-go-go related gene; HPLC, high-performance liquid chromatography; HTS, high-throughput screening; MS, mass spectroscopy; PE, petroleum ether; rt, room temperature; SAR, structure−activity relationship; THF, tetrahydrofuran

■ REFERENCES

(1) WHO. *World Malaria Report 2020*; World Health Organization: Geneva, 2020. ISBN: 978-92-4-156572-1.

(2) Dondorp, A. M.; Nosten, F.; Yi, P.; Das, D.; Phyo, A. P.; Tarning, J.; Lwin, K. M.; Ariey, F.; Hanpithakpong, W.; Lee, S. J.; Ringwald, P.; Silamut, K.; Imwong, M.; Chotivanich, K.; Lim, P.; Herdman, T.; An, S. S.; Yeung, S.; Singhasivanon, P.; Day, N. P. J.; Lindegardh, N.; Socheat, D.; White, N. J. Artemisinin resistance in *Plasmodium falciparum* malaria. *N. Eng. J. Med.* **2009**, *361*, 455−467.

(3) Nsanzabana, C. Resistance to artemisinin combination therapies (ACTs): do not forget the partner drug! *Trop. Med. Infect. Dis.* **2019**, *4*, No. E26.
(4) Wells, T. N. C.; Van Huijsduijnen, R. H.; Van Voorhis, W. C. Malaria medicines: a glass half-full? *Nat. Rev. Drug Discovery* **2015**, *14*, 424−442.
(5) The malERA Refresh Consultative Panel on Insecticide and Drug Resistance. The malERA Refresh Consultative Panel on Insecticide and Drug Resistance. malERA: An updated research agenda for insecticide and drug resistance in malaria elimination and eradication. *PLoS Med.* **2017**, *14*, No. e1002450.
(6) Tse, E. G.; Korsik, M.; Todd, M. H. The past, present and future of anti-malarial medicines. *Malar. J.* **2019**, *18*, No. 93.
(7) Katsuno, K.; Burrows, J. N.; Duncan, K.; Hooft van Huijsduijnen, R.; Kaneko, T.; Kita, K.; Mowbray, C. E.; Schmatz, D.; Warner, P.; Slingsby, B. T. Hit and lead criteria in drug discovery for infectious diseases of the developing world. *Nat. Rev. Drug Discovery* **2015**, *14*, 751−758.
(8) Burrows, J. N.; Duparc, S.; Gutteridge, W. E.; van Huijsduijnen, R. H.; Kaszubska, W.; Macintyre, F.; Mazzuri, S.; Möhrle, J. J.; Wells, T. N. C. New developments in antimalarial target candidate and product profiles. *Malar. J.* **2017**, *16*, No. 26.
(9) Duffy, S.; Avery, V. M. Development and optimization of a novel 384-well anti-malarial imaging assay validated for high-throughput screening. *Am. J. Trop. Med. Hyg.* **2012**, *86*, 84−92.
(10) Nara, H.; Sato, K.; Naito, T.; Mototani, H.; Oki, H.; Yamamoto, Y.; Kuno, H.; Santou, T.; Kanzaki, N.; Terauchi, J.; Uchikawa, O.; Kori, M. Discovery of novel, highly potent, and selective quinazoline-2-carboxamide-based matrix metalloproteinase (MMP)-13 inhibitors without a zinc binding group using a structure-based design approach. *J. Med. Chem.* **2014**, *57*, 8886−8902.
(11) Fingleton, B. MMPs as therapeutic targets−still a viable option? *Semin. Cell Dev. Biol.* **2008**, *19*, 61−68.
(12) Fields, G. B. The rebirth of matrix metalloproteinase inhibitors: moving beyond the dogma. *Cells* **2019**, *8*, No. 984.
(13) Recent example on methylarene scaffold: Shimojo, H.; Moriyama, K.; Togo, H. A one-pot, transition-metal-free procedure for C-O, C-S, and C-N bond formation at the benzylic position of methylarenes. *Synthesis* **2015**, *47*, 1280−1290.
(14) Recent example on methylarene scaffold: Tanaka, S.; Fukui, M.; Otake, K.; Kasai, M.; Shirahase, H. Preparation of Cyclic Compounds, Their Pharmaceutical Compositions, and PTP-1B Inhibitors. WO2014123203A12014.
(15) Fletcher, S.; Avery, V. M. A novel approach for the discovery of chemically diverse anti-malarial compounds targeting the *Plasmodium falciparum* coenzyme A synthesis pathway. *Malar. J.* **2014**, *13*, No. 343.
(16) Leroux, F. Atropisomerism, biphenyls, and fluorine: a comparison of rotational barriers and twist angles. *ChemBioChem* **2004**, *5*, 644−649.
(17) Müller, K.; Faeh, C.; Diederich, F. Fluorine in pharmaceuticals: looking beyond intuition. *Science* **2007**, *317*, 1881−1886.
(18) Jagodzinska, M.; Huguenot, F.; Candiani, G.; Zanda, M. Assessing the bioisosterism of the trifluoromethyl group with a protease probe. *ChemMedChem* **2009**, *4*, 49−51.
(19) Mischlinger, J.; Agnandji, S. T.; Ramharter, M. Single dose treatment of malaria-current status and perspectives. *Expert Rev. Anti-Infect. Ther.* **2016**, *14*, 669−678.
(20) Van Vleet, T. R.; Liu, H.; Lee, A.; Blomme, E. A. G. Acyl glucuronide metabolites: Implications for drug safety assessment. *Toxicol. Lett.* **2017**, *272*, 1−7.
(21) Gunduz, M.; Argikar, U. A.; Cirello, A. L.; Dumouchel, J. L. New perspectives on acyl glucuronide risk assessment in drug discovery: investigation of in vitro stability, in situ reactivity, and bioactivation. *Drug Metab. Lett.* **2018**, *12*, 84−92.
(22) Smith, D. A.; Hammond, T.; Baillie, T. Safety assessment of acyl glucuronides-a simplified paradigm. *Drug Metab. Dispos.* **2018**, *46*, 908−912.
(23) Ishikawa, M.; Hashimoto, Y. Improvement in aqueous solubility in small molecule drug discovery programs by disruption of molecular planarity and symmetry. *J. Med. Chem* **2011**, *54*, 1539−1554.
(24) Boes, A.; Spiegel, H.; Kastilan, R.; Bethke, S.; Voepel, N.; Chudobová, I.; Bolscher, J. M.; Dechering, K. J.; Fendel, R.; Buyel, J. F.; Reimann, A.; Schillberg, S.; Fischer, R. Analysis of the dose-dependent stage-specific in vitro efficacy of a multi-stage malaria vaccine candidate cocktail. *Malar J.* **2016**, *15*, No. 279.
(25) Duffy, S.; Avery, V. M. Identification of inhibitors of *Plasmodium falciparum* gametocyte development. *Malar. J.* **2013**, *12*, No. 408.
(26) Duffy, S.; Loganathan, S.; Holleran, J. P.; Avery, V. M Large-scale production of *Plasmodium falciparum* gametocytes for malaria drug discovery. *Nat. Protoc.* **2016**, *11*, No. 976.
(27) Sanz, L. M.; Crespo, B.; De-Cozar, C.; Ding, X. C.; Llergo, J. L.; Burrows, J. N.; Garcia-Bustos, J. F.; Gamo, F. J. *P. falciparum* in vitro killing rates allow to discriminate between different antimalarial mode-of-action. *PLoS One* **2012**, *7*, No. e30949.
(28) Snyder, C.; Chollet, J.; Santo-Tomas, J.; Scheurer, C.; Wittlin, S. In vitro and in vivo interaction of synthetic peroxide RBx11160 (OZ277) with piperaquine in Plasmodium models. *Exp. Parasitol.* **2007**, *115*, 296−300.
(29) Ashton, T. D.; Devine, S. M.; Möhrle, J. J.; Laleu, B.; Burrows, J. N.; Charman, S. A.; Creek, D. J.; Sleebs, B. E. Development of the most clinically advanced modern antimalarials. *J. Med. Chem.* **2019**, *62*, 10526−10562.
(30) Phillips, M. A.; Lotharius, J.; Marsh, K.; White, J.; Dayan, A.; White, K. L.; Njoroge, J. W.; El Mazouni, F.; Lao, Y.; Kokkonda, S.; Tomchick, D. R.; Deng, X.; Laird, T.; Bhatia, S. N.; March, S.; Ng, C. L.; Fidock, D. A.; Wittlin, S.; Lafuente-Monasterio, M.; Benito, F. J.; Alonso, L. M.; Martinez, M. S.; Jimenez-Diaz, M. B.; Bazaga, S. F.; Angulo-Barturen, I.; Haselden, J. N.; Louttit, J.; Cui, Y.; Sridhar, A.; Zeeman, A. M.; Kocken, C.; Sauerwein, R.; Dechering, K.; Avery, V. M.; Duffy, S.; Delves, M.; Sinden, R.; Ruecker, A.; Wickham, K. S.; Rochford, R.; Gahagen, J.; Iyer, L.; Riccio, E.; Mirsalis, J.; Bathhurst, I.; Rueckle, T.; Ding, X.; Campo, B.; Leroy, D.; Rogers, M. J.; Rathod, P. K.; Burrows, J. N.; Charman, S. A. A long-duration dihydroorotate dehydrogenase inhibitor (DSM265) for prevention and treatment of malaria. *Sci. Transl. Med.* **2015**, *7*, No. 296ra111.
(31) Stickles, A. M.; de Almeida, M. J.; Morrisey, J. M.; Sheridan, K. A.; Forquer, I. P.; Nilsen, A.; Winter, R. W.; Burrows, J. N.; Fidock, D. A.; Vaidya, A. B.; Riscoe, M. K. Subtle changes in endochin-like quinolone structure alter the site of inhibition within the cytochrome bc1 complex of *Plasmodium falciparum*. *Antimicrob. Agents Chemother.* **2015**, *59*, 1977−1982.
(32) Baragaña, B.; Hallyburton, I.; Lee, M. C.; Norcross, N. R.; Grimaldi, R.; Otto, T. D.; Proto, W. R.; Blagborough, A. M.; Meister, S.; Wirjanata, G.; Ruecker, A.; Upton, L. M.; Abraham, T. S.; Almeida, M. J.; Pradhan, A.; Porzelle, A.; Martínez, M. S.; Bolscher, J. M.; Woodland, A.; Luksch, T.; Norval, S.; Zuccotto, F.; Thomas, J.; Simeons, F.; Stojanovski, L.; Osuna-Cabello, M.; Brock, P. M.; Churcher, T. S.; Sala, K. A.; Zakutansky, S. E.; Jiménez-Díaz, M. B.; Sanz, L. M.; Riley, J.; Basak, R.; Campbell, M.; Avery, V. M.; Sauerwein, R. W.; Dechering, K. J.; Noviyanti, R.; Campo, B.; Frearson, J. A.; Angulo-Barturen, I.; Ferrer-Bazaga, S.; Gamo, F. J.; Wyatt, P. G.; Leroy, D.; Siegl, P.; Delves, M. J.; Kyle, D. E.; Wittlin, S.; Marfurt, J.; Price, R. N.; Sinden, R. E.; Winzeler, E. A.; Charman, S. A.; Bebrevska, L.; Gray, D. W.; Campbell, S.; Fairlamb, A. H.; Willis, P. A.; Rayner, J. C.; Fidock, D. A.; Read, K. D.; Gilbert, I. H. A novel multiple-stage antimalarial agent that inhibits protein synthesis. *Nature* **2015**, *522*, 315−320.
(33) Meister, S.; Plouffe, D. M.; Kuhen, K. L.; Bonamy, G. M. C.; Wu, T.; Barnes, S. W.; Bopp, S. E.; Borboa, R.; Bright, A. T.; Jianwei Che, J.; Cohen, S.; Dharia, N. V.; Gagaring, K.; Gettayacamin, M.; Gordon, P.; Groessl, T.; Kato, N.; Lee, M. C. S.; McNamara, C. W.; Fidock, D. A.; Nagle, A.; Nam, T.-G.; Richmond, W.; Roland, J.; Rottmann, M.; Zhou, B.; Froissard, P.; Glynne, R. J.; Mazier, D.; Sattabongkot, J.; Schultz, P. G.; Tuntland, T.; Walker, J. R.; Zhou, Y.; Chatterjee, A.; Diagana, T. T.; Winzeler, E. A. Imaging of Plasmodium liver stages to drive next-generation antimalarial drug discovery. *Science* **2011**, *334*, 1372−1377.

https://doi.org/10.1021/acs.jmedchem.1c00441
J. Med. Chem. XXXX, XXX, XXX−XXX

(34) Paquet, T.; Le Manach, C.; Cabrera, D. G.; Younis, Y.; Henrich, P. P.; Abraham, T. S.; Lee, M. C. S.; Basak, R.; Ghidelli-Disse, S.; Lafuente-Monasterio, M. J.; Bantscheff, M.; Ruecker, A.; Blagborough, A. M.; Zakutansky, S. E.; Zeeman, A. M.; White, K. L.; Shackleford, D. M.; Mannila, J.; Morizzi, J.; Scheurer, C.; Angulo-Barturen, I.; Martinez, M. S.; Ferrer, S.; Sanz, L. M.; Gamo, F. J.; Reader, J.; Botha, M.; Dechering, K. J.; Sauerwein, R. W.; Tungtaeng, A.; Vanachayangkul, P.; Lim, C. S.; Burrows, J.; Witty, M. J.; Marsh, K. C.; Bodenreider, C.; Rochford, R.; Solapure, S. M.; Jimenez-Diaz, M. B.; Wittlin, S.; Charman, S. A.; Donini, C.; Campo, B.; Birkholtz, L. M.; Hanson, K. K.; Drewes, G.; Kocken, C. H. M.; Delves, M. J.; Leroy, D.; Fidock, D. A.; Waterson, D.; Street, L. J.; Chibale, K. Antimalarial efficacy of MMV390048, an inhibitor of Plasmodium phosphatidylinositol 4-kinase. *Sci. Transl. Med.* **2017**, *9*, No. eaad9735.

(35) Jimenez-Díaz, M. B.; Mulet, V.; Viera, S.; Gomez, V.; Garuti, H.; Ibanez, J.; Alvarez-Doval, A.; Shultz, L. D.; Martínez, A.; Gargallo-Viola, D.; Angulo-Barturen, I. Improved murine model of malaria using *Plasmodium falciparum* competent strains and non-myelodepleted NOD-scid IL2Rgammanull mice engrafted with human erythrocytes. *Antimicrob. Agents Chemother.* **2009**, *53*, 4533−4536.

(36) Terauchi, J.; Kuno, H.; Nara, H.; Oki, H.; Sato, K. Preparation of Heterocyclic Amides as MMP-13 Inhibitors for Treating Osteoarthritis and Rheumatoid Arthritis. WO2005105760A12005.

(37) Charman, S. A.; Andreu, A.; Barker, H.; Blundell, S.; Campbell, A.; Campbell, M.; Chen, G.; Chiu, F. C. K.; Crighton, E.; Katneni, K.; Morizzi, J.; Patil, R.; Pham, T.; Ryan, E.; Saunders, J.; Shackleford, D. M.; White, K. L.; Almond, L.; Dickins, M.; Smith, D. A.; Moehrle, J. J.; Burrows, J. N.; Abla, N. An in vitro toolbox to accelerate anti-malarial drug discovery and development. *Malar. J.* **2020**, *19*, No. 1.

(38) Bevan, C. D.; Lloyd, R. S. A high-throughput screening method for the determination of aqueous drug solubility using laser nephelometry in microtiter plates. *Anal Chem.* **2000**, *72*, 1781−1787.

(39) Jantratid, E.; Janssen, N.; Reppas, C.; Dressman, J. B. Dissolution media simulating conditions in the proximal human gastrointestinal tract: An update. *Pharm. Res.* **2008**, *25*, 1663−1676.

https://doi.org/10.1021/acs.jmedchem.1c00441
J. Med. Chem. XXXX, XXX, XXX−XXX